



**HAL**  
open science

## **Cobalt and marine redox evolution**

Elizabeth Swanner, Noah Planavasky, Stefan Lalonde, Leslie Robbins, Andrey Bekker, Olivier J. Rouxel, Mak A. Saito, Andreas Kappler, Stephen J. Mojzsis, Kurt O. Konhauser

► **To cite this version:**

Elizabeth Swanner, Noah Planavasky, Stefan Lalonde, Leslie Robbins, Andrey Bekker, et al.. Cobalt and marine redox evolution. *Earth and Planetary Science Letters*, 2014, 390, pp.253-263. 10.1016/j.epsl.2014.01.001 . insu-01024353

**HAL Id: insu-01024353**

**<https://insu.hal.science/insu-01024353>**

Submitted on 8 Mar 2021

**HAL** is a multi-disciplinary open access archive for the deposit and dissemination of scientific research documents, whether they are published or not. The documents may come from teaching and research institutions in France or abroad, or from public or private research centers.

L'archive ouverte pluridisciplinaire **HAL**, est destinée au dépôt et à la diffusion de documents scientifiques de niveau recherche, publiés ou non, émanant des établissements d'enseignement et de recherche français ou étrangers, des laboratoires publics ou privés.

## Cobalt and marine redox evolution

Elizabeth D. Swanner<sup>a, \*</sup>, Noah J. Planavsky<sup>b</sup>, Stefan V. Lalonde<sup>c</sup>, Leslie J. Robbins<sup>d</sup>, Andrey Bekker<sup>e</sup>,  
 Olivier J. Rouxel<sup>f</sup>, Mak A. Saito<sup>g</sup>, Andreas Kappler<sup>a</sup>, Stephen J. Mojzsis<sup>h, i, j</sup>, Kurt O. Konhauser<sup>d</sup>

<sup>a</sup> Eberhard-Karls University Tübingen, Sigwartstrasse 10, 72076 Tübingen, Germany

<sup>b</sup> Yale University, New Haven, CT 06520, USA

<sup>c</sup> European Institute for Marine Studies, Technopôle Brest-Iroise, 29280 Plouzané, France

<sup>d</sup> University of Alberta, Edmonton, Alberta, T6G 2E3, Canada

<sup>e</sup> University of Manitoba, Winnipeg, Manitoba, R3T 2N2, Canada

<sup>f</sup> IFREMER, Centre de Brest, Technopôle Brest-Iroise, 29280 Plouzané, France

<sup>g</sup> Woods Hole Oceanographic Institution, Woods Hole, MA 02543, USA

<sup>h</sup> Ecole Normale Supérieure de Lyon and Université Claude Bernard Lyon 1, CNRS UMR 5276, 2 rue Raphaël Dubois, 69622 Villeurbanne, France

<sup>i</sup> Hungarian Academy of Sciences, Institute for Geological and Geochemical Research, 45 Budaörsi Street, H-1112 Budapest, Hungary

<sup>j</sup> University of Colorado, UCB 399, 2200 Colorado Avenue, Boulder, CO 80309-0399, USA

\*: Corresponding author : Elizabeth D. Swanner, tel.: +49 (0) 7071 29 73061 ;

email address : [elizabeth.swanner@ifg.uni-tuebingen.de](mailto:elizabeth.swanner@ifg.uni-tuebingen.de)

### Abstract:

Cobalt (Co) is a bio-essential trace element and limiting nutrient in some regions of the modern oceans. It has been proposed that Co was more abundant in poorly ventilated Precambrian oceans based on the greater utilization of Co by anaerobic microbes relative to plants and animals. However, there are few empirical or theoretical constraints on the history of seawater Co concentrations. Herein, we present a survey of authigenic Co in marine sediments (iron formations, authigenic pyrite and bulk euxinic shales) with the goal of tracking changes in the marine Co reservoir throughout Earth's history. We further provide an overview of the modern marine Co cycle, which we use as a platform to evaluate how changes in the redox state of Earth's surface were likely to have affected marine Co concentrations. Based on sedimentary Co contents and our understanding of marine Co sources and sinks, we propose that from ca. 2.8 to 1.8 Ga the large volume of hydrothermal fluids circulating through abundant submarine ultramafic rocks along with a predominantly anoxic ocean with a low capacity for Co burial resulted in a large dissolved marine Co reservoir. We tentatively propose that there was a decrease in marine Co concentrations after ca. 1.8 Ga resulting from waning hydrothermal Co sources and the expansion of sulfide Co burial flux. Changes in the Co reservoir due to deep-water ventilation in the Neoproterozoic, if they occurred, are not resolvable with the current dataset. Rather, Co enrichments in Phanerozoic euxinic shales deposited during ocean anoxic events (OAE) indicate Co mobilization from expanded anoxic sediments and enhanced hydrothermal sources. A new record of marine Co concentrations provides a platform from which we can reevaluate the role that environmental Co concentrations played in shaping biological Co utilization throughout Earth's history.

**Highlights** : ► Authigenic iron oxides and pyrite record marine Co concentrations. ► The Precambrian marine Co reservoir was greatest from 2.8–1.84 Ga. ► Sedimentary Co enhancements are linked to anoxia and hydrothermal activity. ► A Neoproterozoic drop in the marine Co reservoir with ventilation is not resolvable. ► The marine Co reservoir broadly corresponds to acquisition of Co-binding proteins.

**Keywords**: cobalt ; trace element proxies ; ocean redox ; shale ; iron formation ; pyrite

**Abbreviations** : Co, cobalt ; Fe, iron ; Mn, manganese ; IF, iron formation ; OMZ, oxygen minimum zone ; OAE, oceanic anoxic event ; MAR, mass accumulation rate

## 64 1. Introduction

65 The availability of bio-essential trace elements such as Fe, Mo, Zn, Co, Ni, and Cu  
66 underpins the emergence, long-term evolution, and activity of life on our planet. The  
67 record of trace element utilization imprinted in modern organisms is commonly thought  
68 to reflect metal availability in seawater when key metalloproteins evolved (Dupont et al.,  
69 2006; Fraústo da Silva and Williams, 2001; Zerkle et al., 2005). The availability and  
70 removal of trace elements within aqueous habitats for life reflects the compositional  
71 evolution of the Earth's crust, but is also controlled by redox changes driven by  
72 metabolic innovation (Anbar, 2008). Temporal patterns in the concentrations and  
73 isotopic variations of trace elements in ancient sediments can serve as proxies for major  
74 changes in redox conditions in the oceans and atmosphere over geologic timescales  
75 (Anbar, 2008; Konhauser et al., 2009; Scott et al., 2008; Scott et al., 2012), and can  
76 provide a means to test the idea that environmental availability controlled the  
77 evolutionary history of metal utilization. However, empirical records of metal variation  
78 through time have only been described for a few trace elements. For some elements  
79 (e.g., Mo), the geochemical and biological records roughly converge on and support the  
80 interpretation of limited availability and biological utilization for early organisms (David  
81 and Alm, 2011; Scott et al., 2008). For other metals, the records do not match so well.  
82 For instance, Zn is an especially important yet relatively late adoption in eukaryotic  
83 metal-binding protein domains. As such, it was believed that Zn was relatively scarce in  
84 seawater until the Neoproterozoic when the oceans became fully oxygenated (Dupont  
85 et al., 2006). Yet, surprisingly, Zn abundance in the oceans appears to have been  
86 relatively constant throughout much of Earth's history (Scott et al., 2012), and Zn

87 bioavailability may have been limited by the formation of soluble complexes with  
88 organics or sulfide (Robbins et al., 2013). Similarly, Ni concentrations were elevated in  
89 Archean seawater (Kamber, 2010; Konhauser et al., 2009), yet the proteomic record  
90 suggests increasing post-Archean biological Ni utilization (e.g. David and Alm, 2011).  
91 Genomic reconstructions support the early biological utilization of Co (David and Alm,  
92 2011; Dupont et al., 2006), perhaps reflecting an ancient abundance of dissolved  
93 marine Co relative to the modern oceans. However, this model has not yet been tested  
94 against the geological record.

95 Cobalt is a bio-essential metal for life, forming amongst others, the central cobalt-  
96 corrin complex of cobalamin (vitamin B<sub>12</sub>). Eukaryotes use Co primarily as cobalamin in,  
97 for example, methionine synthesis. Bacteria and archaea additionally use cobalamin in  
98 enzymes for anaerobic metabolisms, including fermentation, dehalogenation, and one-  
99 carbon compound electron transfers (Banerjee and Ragsdale, 2003). Direct binding of  
100 Co also occurs in enzymes such as nitrile hydratase, used in amide metabolism. Cobalt  
101 can also substitute for Zn in carbonic anhydrase, an enzyme responsible for  
102 interconversion of CO<sub>2</sub> and bicarbonate in some phytoplankton, suggesting that marine  
103 Co availability is important in regulating the global carbon cycle (Morel et al., 1994).

104 Cobalt concentrations in modern seawater vary from 3 to 120 pM (Saito and Moffett,  
105 2002), with variations dependent on interactions with other metals, biota and organic  
106 matter. Cobalt shows nutrient-like behavior with surface minimum concentrations due to  
107 biological uptake by phytoplankton (Saito et al., 2010; Saito and Moffett, 2002). Yet  
108 strong Co ligands complex nearly all of the dissolved Co in some oligotrophic waters  
109 (Noble et al., 2008; Saito, 2004; Saito and Moffett, 2001; Saito et al., 2005), although

110 some portion of this complexed Co pool is likely bioavailable (Saito, 2004; Saito and  
111 Moffett, 2001). In coastal and deep waters, Co behaves as a scavenged-type element  
112 (Moffett and Ho, 1996; Saito, 2004), becoming oxidized and adsorbed to Mn(III,IV)  
113 oxides as they precipitate (Murray and Dillard, 1979). Co scavenging is thought to be  
114 catalyzed by Mn(II)-oxidizing bacteria (Moffett and Ho, 1996; Murray et al., 2007).

115 Previous estimates of marine Co concentrations through Earth's history were based  
116 on thermodynamic considerations and assumptions regarding evolving marine redox  
117 and chemical composition (Saito et al., 2003), and did not consider how some key  
118 sources and sinks changed through time. Furthermore, equilibrium mineral precipitation  
119 models neglect kinetic control over precipitation. In this study, we use the sedimentary  
120 record of Co to track first-order changes in the marine Co reservoir through time, along  
121 with estimated magnitudes of the modern sources and sinks to infer the causes for Co  
122 reservoir change. We also suggest that the contents of Co of authigenic marine pyrite  
123 can be used as a proxy for marine Co concentrations.

124

## 125 **2. Behavior of Co in marine environments**

126 The formation of authigenic marine phases is subject to thermodynamic control,  
127 based on the abundance and speciation of ions, redox, and pH conditions. However,  
128 kinetically-driven scavenging reactions also influence the composition of marine  
129 precipitates. As a basis for the discussion below, Eh-pH diagrams detailing Co  
130 speciation were generated with the Act2 module of Geochemists' Workbench using the  
131 Minteq thermodynamic database from 2005. Cobalt(II) was set to 100 nM, Fe(II) and  
132 Mn(II) to 50  $\mu$ M, bicarbonate to 5 mM, silica to 2.2 mM (saturation with amorphous

133 silica; Konhauser et al., 2007) in seawater ionic strength; physical constraints were  
134 25°C and 1 atmosphere ambient pressure. Cobalt does not form carbonate compounds,  
135 and  $\text{Co(OH)}_3$  precipitates are only possible at very high Eh-pH conditions (**Fig. 1**).  
136 Cobalt(II) is oxidized to Co(III) in the same Eh-pH space where Mn(II) oxidation occurs,  
137 accounting for the oxidation of Co(II) and adsorption of Co(III) to precipitated Mn(III,IV)  
138 oxides (Murray and Dillard, 1979; Takahashi et al., 2007). Iron(II) is oxidized to Fe(III) at  
139 a lower redox potential than Co(II) and Mn(II) at marine pH (~8).

140 Adsorption of Co(II) and Co(III) to surface sites on Fe(III) (oxyhydr)oxides (Musić et  
141 al., 1979) and Mn(III,IV) oxides (Takahashi et al., 2007), respectively, is an important  
142 pathway for scavenging of Co under oxic conditions (Koschinsky and Hein, 2003;  
143 Stockdale et al., 2010; Takahashi et al., 2007). Soluble Co maxima occur below the  $\text{O}_2$ -  
144  $\text{H}_2\text{S}$  chemocline in modern euxinic basins in conjunction with both the soluble Fe and  
145 Mn peaks (Dryssen and Kremling, 1990; Öztürk, 1995; Viollier et al., 1995), which  
146 indicates that Co is released by reductive dissolution of both Mn(III,IV) oxides and  
147 Fe(III) (oxyhydr)oxides. Both poorly crystalline and crystalline Fe(III) (oxyhydr)oxide  
148 surfaces efficiently scavenge Co(II) in waters with pH above ~7 (Borggaard, 1987;  
149 Gunnarsson et al., 2000; Musić et al., 1979; Dzombak and Morel, 1990), likely as  
150 bidentate inner-sphere complexes (Beak et al., 2011), while Co(III) is substituted for Mn  
151 in Mn(III/IV) oxides (Manceau et al., 1997). Correlation between Co and Fe in  
152 hydrothermal sediments collected from Endeavor Segment, Juan de Fuca (**Fig. 2**; data  
153 from Hrishceva and Scott, 2007) implies a common delivery path for both metals and is  
154 consistent with an Fe(III) (oxyhydr)oxide Co shuttle.

155 Sorption of Co(II) to ferrihydrite, likely the dominant Co scavenging pathway in

156 Fe(II)-rich seawater (e.g. Konhauser et al., 2009), was investigated with MINTEQ using  
157 constants and site densities previously determined for ferrihydrite (Dzombak and Morel,  
158 1990). Activities of dissolved components were corrected using the Davies equation,  
159 and modeling utilized 100 pM initial Co(II), 0.56M NaCl electrolyte to simulate seawater,  
160 and 1 g/L free ferrihydrite mineral (a constant concentration of surface sites during  
161 steady-state production of ferrihydrite). We compared Co sorption with and without Co  
162 ligands at modern (ca. 40 pM; Saito, 2004; Saito and Moffett, 2001) and high (400 pM)  
163 concentrations to investigate whether Co ligands prevent sorption of Co(II) to surface  
164 sites of ferrihydrite. The amount of Co(II) sorbed was unaffected at marine pH with 40  
165 pM ligands , but Co(II) sorption to ferrihydrite was negligible when ligand concentrations  
166 were 400 pM (**Fig. 3**). We note that this model utilizes data for ligands specific to Co(II),  
167 but Co(III)-ligand complexes are likely extremely inert (Saito et al., 2005), and should  
168 further decrease the pool of Co available for metal sorption. We also did not examine  
169 the effects of inorganic species(e.g. Si), which can compete with metals for surface  
170 binding sites on ferrihydrite (Konhauser et al., 2007; Konhauser et al., 2009). As  
171 illustrated by those studies, the presence of Si should lower the amount of metal bound  
172 for any given dissolved Co concentration.

173 In oligotrophic surface waters, Co concentrations are controlled by phytoplankton  
174 uptake and binding to organic ligands (Saito and Moffett, 2001, 2002) rather than by the  
175 scavenging reactions with Mn that occur in coastal and deep waters (Moffett and Ho,  
176 1996). Cobalt concentrations in phytoplankton are similar to abundances of Cd and Cu  
177 and enriched by as much as 10x over Mo (Ho et al., 2003). Organic material can also  
178 sorb trace elements and transfer them to sediments (Broecker and Peng, 1982;

179 Krauskopf, 1956), although this process is not as quantitatively significant for Co as it is  
180 for other metals (e.g., Cd, Zn; Algeo and Maynard, 2004; Yee and Fein, 2003).

181 The formation of sulfide minerals governs the concentrations of Co in anoxic and  
182 sulfidic waters. Cobalt sulfide is more soluble than sulfides of some other biologically  
183 important elements (e.g. Cu, Zn; Saito et al., 2003), and dissolved Co concentrations  
184 below the chemocline of sulfidic waters can exceed average ocean concentrations by  
185 several orders of magnitude (Dryssen and Kremling, 1990; Viollier et al., 1995).  
186 Previous calculations suggested that the formation of Co-sulfide should scavenge  
187 dissolved Co from sulfidic waters (Dryssen and Kremling, 1990; Kremling, 1983), but  
188 little evidence exists for this particulate Co phase (Saito et al., 2003). However, field  
189 observations show that some Co remains dissolved in sulfidic waters, while less soluble  
190 metals (e.g., Cu, Cd) are rapidly removed (Öztürk, 1995; Viollier et al., 1995). The  
191 exchange of the bisulfide ion with water molecules hydrating dissolved Co(II) is slower  
192 than with those hydrating Fe(II), likely contributing to the persistence of dissolved Co(II)  
193 in sulfidic waters (Morse and Luther III, 1999). For most sulfidic marine systems, this  
194 means that while FeS is more soluble than CoS (e.g. Saito et al., 2003), FeS formation  
195 is kinetically favored, and Co is incorporated into FeS rather than precipitating as CoS  
196 (Huerta-Diaz and Morse, 1992; Morse and Arakaki, 1993).

197 The concentration of metals, including Co, in sulfidic waters is also buffered by the  
198 formation of soluble metal-sulfide complexes (Daskalakis and Helz, 1992), although this  
199 seems to be more important for metals such as Cd, Zn, and Cu that form stronger  
200 sulfide complexes. However, above 1  $\mu\text{M}$  total sulfide, soluble Co-sulfide complexes will  
201 reduce the dissolved Co(II) pool (Saito et al., 2003). Regardless of the initial phase of

202 aqueous precipitate, Co ultimately substitutes into pyrite during sedimentary diagenesis  
203 (Huerta-Diaz and Morse, 1992; Stockdale et al., 2010).

204

### 205 **3. Marine Co sources and sinks**

206 The concentration of elements in seawater reflects a balance between delivery and  
207 removal of elements via precipitation and adsorption processes (e.g. Broecker, 1971;  
208 Krauskopf, 1956). To quantitatively interpret changes in the marine Co reservoir, as  
209 recorded by sediments deposited under different redox conditions, we detail below  
210 estimates of the fluxes of dissolved Co to seawater, and mass accumulation rates  
211 (MAR) for sediments deposited under oxic, anoxic and euxinic conditions (**Table 1**).

212

#### 213 *3.1 Marine Co sources*

214 The amount of Co present in the crust ultimately governs the amount of Co delivered  
215 to the oceans through fluid-rock interaction. Minerals with higher Fe, Mg, and Cr  
216 contents are also enriched in Co (Carr and Turekian, 1961), specifically olivine and  
217 pyroxene present in ultramafic rocks (Glassley and Piper, 1978). Dissolved Co is  
218 delivered to seawater via rivers and hydrothermal fluids that source Co predominantly  
219 from mafic and ultramafic rocks. The estimated riverine flux of Co is  $5.5 \times 10^{12}$  g kyr<sup>-1</sup>  
220 (**Table 1**; Gaillardet et al., 2003). Cobalt fluxes from the continents were likely higher  
221 prior to 2.5 Ga due to their more mafic compositions, after which average Co  
222 concentrations in the continental crust dropped from 22 to 15 ppm (Condie, 1993). Dust  
223 can add dissolved Co to surface waters, but this process is likely to be minor and  
224 geographically and seasonally restricted (Shelley et al., 2012).

225 Although recent work has highlighted the role of hydrothermal fluids in supplying  
226 scavenged-type elements to the ocean reservoir (e.g. Fe; Saito et al., 2013; Tagliabue  
227 et al., 2010), initial measurements have found little evidence for Co fluxes from  
228 hydrothermal systems to seawater (Noble et al., 2012; Noble et al., 2008). However,  
229 hydrothermal fluids contain Co in concentrations often several orders of magnitude  
230 above average seawater (Metz and Trefry, 2000), implying that delivery of hydrothermal  
231 Co to open oceans is limited by efficient, near-field scavenging reactions in oxic  
232 seawater (German et al., 1991). Using the fluid flow volume through high- and low-  
233 temperature hydrothermal systems as estimated from the oceanic Mg budget by  
234 Elderfield and Schultz (1996), we calculated Co fluxes out of both types of systems as  
235 described by Reinhard et al. (2013). The Co anomaly for high-temperature systems  
236 utilized the difference between concentrations within the Plume vent on the Juan de  
237 Fuca Ridge ( $200 \text{ nmol kg}^{-1}$  at  $246^\circ\text{C}$ ) and bottom waters ( $0.02 \text{ nmol kg}^{-1}$ ; Metz and  
238 Trefry, 2000). The Co anomaly for low-temperature systems was based on Co data  
239 from site 1027 on the Juan de Fuca Ridge ( $0.7 \text{ nmol kg}^{-1}$  at  $64^\circ\text{C}$ ) relative to bottom  
240 waters ( $0.03 \text{ nmol kg}^{-1}$ ; Wheat et al., 2003). We estimate a total hydrothermal Co flux of  
241  $1.2 \times 10^{11} \text{ g Co kyr}^{-1}$ ; 2.4% of total the total Co flux (**Table 1**). We recognize that the net  
242 fluxes of most hydrothermally derived metals to the open ocean remain poorly  
243 constrained; metals released from hydrothermal vents are readily incorporated into  
244 sulfide or oxide precipitates within plumes, thereby diminishing dispersion. However,  
245 nanoparticulate sulfides or organic ligands may stabilize and transport trace elements  
246 away from vents (Sander and Koschinsky, 2011; Toner et al., 2009; Yucel et al., 2011),  
247 increasing trace element, and probably Co, fluxes to the global ocean. We therefore

248 anticipate that global fluxes of Co from hydrothermal systems will be refined in the near  
249 future (e.g. GEOTRACES).

250

### 251 *3.2 Oxic sedimentary Co sinks*

252 In sediments where oxygen penetrates at least 1 cm, authigenic Fe(III)  
253 (oxyhydr)oxides, Mn(III/IV) oxides and associated Co are permanently buried  
254 (Brumsack, 1989; Froelich et al., 1979). Any Fe(II) and Mn(II) released during  
255 dissimilatory microbial reduction is reoxidized and immobilized before diffusing out of  
256 sediments. Deposition of phytoplankton biomass may also add Co to oxic sediments  
257 (Saito, 2004). Regardless of the pathway for authigenic Co delivery to sediments, Co  
258 released during early diagenesis is immobilized by scavenging with Fe(III)  
259 (oxyhydr)oxides and Mn(III/IV) oxides. Cobalt fluxes to oxic continental margin and  
260 hydrothermal sediments are likely higher than those in the deep sea (Douglas and  
261 Adeney, 2000; Koschinsky and Hein, 2003), but these fluxes are not well-constrained.  
262 Therefore, we use an estimate of  $2.3\text{-}5 \mu\text{g Co cm}^{-3} \text{ kyr}^{-1}$  (Krishnaswami, 1976) from  
263 deep-sea pelagic sediments for an average authigenic oxic Co MAR.

264

### 265 *3.3 Euxinic sedimentary Co sinks*

266 Modern sulfidic (sulfide in porewaters) or euxinic (sulfide in bottom waters)  
267 environments include basins where authigenic Fe(III) (oxyhydr)oxides and Mn(III/IV)  
268 oxides are reductively dissolved below the  $\text{O}_2\text{-H}_2\text{S}$  transition zone, releasing associated  
269 Co (Dryssen and Kremling, 1990; Öztürk, 1995; Viollier et al., 1995). To estimate an

270 euxinic Co MAR, we subtracted the average terrigenous Co/Al ratio ( $198 \mu\text{g g}^{-1}$ ) from  
271 the Co/Al ratio of euxinic sediments ( $204 \mu\text{g g}^{-1}$ ; within errors) from the perennially  
272 euxinic Cariaco basin near Venezuela (Piper and Dean, 2002). Utilizing an average  
273 sedimentation rate, density, and porosity for euxinic Cariaco sediments (Lyons et al.,  
274 2003), our estimated euxinic Co MAR is  $5 \mu\text{g Co cm}^{-3} \text{ kyr}^{-1}$  (**Table 1**). We acknowledge  
275 that there are large errors in this estimate, and higher euxinic Co MAR are observed in  
276 restricted basins (Brumsack, 1989; Hetzel et al., 2009). Although Co is likely enriched  
277 above detrital levels in euxinic sediments, there is almost an order of magnitude lower  
278 enrichment than metals that form strong sulfide complexes (e.g., Mo), which can be  
279 enriched up to 100x above concentrations in oxic sediments (Algeo and Maynard,  
280 2004). Cobalt MAR in euxinic sediments below open marine conditions ( $5 \mu\text{g Co cm}^{-3}$   
281  $\text{kyr}^{-1}$ ) are similar to Co MAR in oxic marine sediments ( $2.3$  to  $5 \mu\text{g Co cm}^{-3} \text{ kyr}^{-1}$ ), in  
282 contrast to Mo (see Scott et al., 2008), demonstrating that expansion of euxinic  
283 sediments at the expense of oxic sediments, or vice versa, should not result in major  
284 changes to the Co reservoir.

285

#### 286 *3.4 Anoxic sedimentary Co sinks*

287 In anoxic marine sediments lacking dissolved sulfide, Fe(III) (oxyhydr)oxides and  
288 Mn(III/IV) oxides are subject to dissimilatory microbial reduction. Fluxes of Co(II) and  
289 Mn(II) have been observed out of sediments underlying oxygen- and sulfide-poor  
290 bottom water (Brumsack, 1989; Saito, 2004), and plumes of dissolved Co mobilized  
291 from anoxic sediments have been observed over oxygen minimum zones (OMZs; Noble  
292 et al., 2012), demonstrating the mobility of Co under anoxic conditions. While

293 remobilization under anoxic conditions is an important source of Co in some coastal  
294 environment, this process does not represent an exogenous supply of Co, and so we  
295 have not included reducing sediments as a source in flux estimates. Because Co is  
296 readily mobilized from anoxic sediments, there is no significant flux of Co to anoxic  
297 sediments, and Co in anoxic sediments solely reflects what is added with detrital  
298 minerals (Brumsack, 1989; van der Weijden et al., 2006). Thus, a decrease in the extent  
299 of anoxic sediments at the expense of oxic or euxinic sediments will decrease the size  
300 of dissolved Co reservoir, while expansion of anoxic sediments should increase the size  
301 of the reservoir.

302 Generally speaking, sediments deposited under an anoxic but non-sulfidic water  
303 column, which are often referred to as ferruginous sediments, are also unlikely to  
304 permanently remove Co. Rare in the modern but common in the Precambrian,  
305 ferruginous sediments are characterized by overlying water column with anoxic  
306 conditions with Fe(II) as the main redox buffer (Planavsky et al., 2011). These redox  
307 conditions also allowed for the deposition of iron formations (IF), which are likely to be a  
308 significant Co sink (**Fig. 4**). However, IFs reflect stabilization of Fe(III) (oxyhydr)oxides  
309 under anoxic conditions where there was anomalously high local Fe(III) fluxes.  
310 Furthermore, most oxide facies IF are found in deep water settings, and oxides are  
311 preserved due to a lack of sufficient organic carbon to drive complete Fe(III) reduction  
312 (Konhauser et al., 2005). Therefore, IF likely have higher capacities for Co burial (with  
313 authigenic Fe(III) (oxyhydr)oxides) than modern anoxic sediments, although IFs  
314 represent a small fraction of overall marine ferruginous settings.

315

#### 316 **4. Archives of Marine Co concentrations**

317 We propose that sedimentary Co concentrations can serve as an archive of marine  
318 Co concentrations. We use this premise to evaluate how key sources and sinks for Co  
319 have varied through time. This compilation also informs the evolution of marine redox  
320 conditions. We focus on two types of sedimentary archives: those in which Co was  
321 sequestered by authigenic Fe(III) (oxyhydr)oxides (IF database), or by iron sulfides  
322 (sedimentary pyrite and euxinic shale databases).

323

##### 324 *4.1 Iron formations as a Co archive*

325

326 Iron(III) (oxyhydr)oxides, generally thought to be the precursor phases to most IF,  
327 have extremely large and reactive surfaces that extensively adsorb cations, including  
328 Co(II), at marine pH (Dzombak and Morel, 1990). Therefore, we propose that the record  
329 of authigenic Co enrichment in IF can be used to evaluate large-scale changes in  
330 marine Co concentrations through time. Similar chemical principles justified using Ni, P,  
331 Cr and Zn enrichments in IF to track changes in seawater concentrations of these  
332 elements (Konhauser et al., 2011; Konhauser et al., 2009; Planavsky et al., 2010b;  
333 Robbins et al., 2013). Precambrian IF are chemical precipitates with minor detrital input.  
334 Authigenic, but diagenetically and metamorphically altered, Fe-rich (hematite, magnetite,  
335 siderite) and Si-rich (quartz) phases dominate the mineralogy of IF, and so their trace  
336 element composition is often inferred to reflect input of these elements from authigenic  
337 vs. detrital phases. Post-depositional alteration of the primary trace element seawater  
338 signatures is generally minimal unless IF have experienced hydrothermal alteration or  
339 near surface weathering (Bau and Moeller, 1993).

340 Historically, Precambrian IF are divided into Algoma-type, which have a spatially  
341 limited extent and formed in proximity to volcanic and hydrothermal settings, and  
342 Superior-type, which are more extensive and where deposited under marine conditions  
343 on a continental shelf or an isolated basin. Both deposits are represented in our dataset  
344 and we assign each IF as being Algoma- or Superior-type for simplicity; in reality there  
345 is a gradation between these IF types (see Bekker et al., 2010). Large, basin-scale IF  
346 deposition experienced a hiatus in the Middle Proterozoic, and a return to IF deposition  
347 in the Neoproterozoic was followed by permanent cessation of IF deposition. The lack of  
348 IF in intervening intervals is evident in our compilation. We further utilize exhalite  
349 deposits and oolitic ironstones to extend the record of Co burial with authigenic Fe oxide  
350 facies into the Phanerozoic.

351 We utilize an expanded dataset of Konhauser et al. (2011; 2009), comprising  
352 published values as well as new data acquired by bulk analysis and *in situ* LA-ICP-MS.  
353 **Supplementary Table 1** reports Co, Al, Ti, Fe, Mn, and S concentrations (where  
354 available) for the 1353 Co data points used in this study. The supplementary information  
355 also includes references for the published data and the descriptions of iron formations  
356 analyzed in this study.

357

#### 358 *4.2 Pyrite as a Co archive*

359 The partitioning of Co into iron sulfide phases is dependent on Co and Fe  
360 concentrations, but importantly for our purposes, it appears to be largely independent of  
361 the amount of hydrogen sulfide (Morse and Arakaki, 1993). In most sulfidic  
362 environments, dissolved  $\text{Fe}^{2+}$  concentrations are near levels predicted from equilibrium

363 with the amorphous Fe-S phase mackinawite (e.g. Helz et al., 2011). Finally, silicate  
364 phases react with sulfide  $10^8$ X more slowly than Fe(III) (oxyhydr)oxide minerals  
365 (Canfield et al., 1992), so Co in detrital minerals should not contribute to Co  
366 concentrations in pyrite. Therefore, it is reasonable to assume that the degree of  
367 authigenic Co enrichment in sediments deposited below euxinic waters should, to a first  
368 order, reflect the dissolved Co concentrations in the water column.

369 In order to use trace element concentrations within pyrite as proxies for seawater  
370 concentrations during sediment deposition, it is essential that (1) pyrites formed within  
371 the sediments that host them, and (2) the metal inventory of pyrite was not overprinted  
372 by secondary alteration processes. In the absence of free oxygen in the Archean  
373 atmosphere, detrital pyrite was delivered to marine sediments (Rasmussen and Buick,  
374 1999). Therefore, only sulfides with early diagenetic textures (e.g. nodules or  
375 disseminated grains) from shales with abundant organic carbon and sulfur and were  
376 included in this study (Rouxel et al., 2005), although not all of the sediments included in  
377 this study have been definitively demonstrated to have been deposited under euxinic  
378 conditions. Post-depositional disturbances to metal content were screened by selecting  
379 samples with no obvious sign of alteration (Rouxel et al., 2005; Rouxel et al., 2006)

380 Individual pyrite grains from black shales were digested and trace element data were  
381 acquired by Thermo Element2 HR-ICP-MS at Woods Hole Oceanographic Institution as  
382 described by Rouxel et al. (2005). A basic description of each sample, as well as the  
383 geological setting and age constrains for the host rock, are reported by Rouxel et al.  
384 (2005). Previously unreported samples include Devonian-age black shales from the  
385 Illinois basin, pyrite nodules from the ca. 1.8 Ga Gunflint Formation of Kakabeca Falls in

386 Ontario, Canada, and pyrite from the ca. 2.7 Ga Manjeri Formation of the Belingwe Belt,  
387 Zimbabwe. Cobalt concentrations are reported in **Supplementary Table 2**. Trace  
388 element compositions of pyrite from modern anoxic sediments are taken from Huerta-  
389 Diaz and Morse (1992) and reference cited therein.

390

#### 391 4.3 *Bulk euxinic shales as a Co archive*

392 Cobalt is enriched in sediments deposited under euxinic conditions (Algeo and  
393 Maynard, 2004), and the shales used in this study have Mo contents >25 ppm,  
394 consistent with euxinia (Scott and Lyons, 2012). Authigenic Co was distinguished from  
395 detrital Co via normalization to a conservative element, in this case Al. This approach is  
396 justified as the Co/Al ratio of fine-grained material derived from continents has varied  
397 little through time (Condie, 1993), and is similar amongst several compilations (Condie,  
398 1993; Kamber et al., 2005; Wedephol, 1971). The Co and Al values for euxinic  
399 sediments used in this study have all been previously published (see **Supplementary**  
400 **references**). Because it is not always straightforward to distinguish detrital from  
401 authigenic trace elements in shales (e.g. Van der Weijden, 2002), we emphasize that  
402 the IF and pyrite datasets are likely to be the most robust indicators of the marine  
403 reservoir.

404

#### 405 4.4 *Statistical analysis of Co datasets*

406 When grouped by ages that correspond to global events (described below), Co  
407 concentrations were log-normally distributed. The statistical differences between  
408 average time-binned values were compared using an unpaired t-test of log

409 concentration values. The  $p$  values for these comparisons are reported in **Table 2**. The  
410 mean and one standard deviation (SD) of log concentration values were then back-  
411 transformed to concentration values, and these are reported as mean ( $\mu\text{g g}^{-1}$ )  $\cdot$  / SD in  
412 accordance with the multiplicative nature of a log-normal distribution (Limpert et al.,  
413 2001).

414

## 415 **5. Evolution of the marine Co reservoir**

### 416 *5.1 Reconstructing changes in Co sources and sinks through Earth history*

417 The datasets of Co in IF, pyrite and shale reveal time-resolved patterns in the  
418 delivery of Co to marine sediments, and thereby indicate first-order changes to the  
419 marine Co reservoir through time (**Fig. 4**). The average Co/Ti ( $\mu\text{g g}^{-1}$ ) of IF  $\geq 2.80$  Ga  
420 (79.85  $\cdot$  / 1.72) are significantly lower than IF deposited between 2.75 to 1.88 Ga (150.57  
421  $\cdot$  / 2.67). Average values then significantly drop in IF, exhalite, and oolitic ironstones  
422 deposited between 1.72 Ga and modern times (62.25  $\cdot$  / 1.84; **Table 2**), despite that  
423 exhalites are prime records of locally derived hydrothermal Co. There is also a  
424 significant difference between the average concentrations of Co (ppm) in pyrites from  
425 shales deposited between 2.8 and 1.84 Ga (7.34  $\cdot$  / 1.77) and those deposited from 1.8  
426 to 0.3 Ga (3.87  $\cdot$  / 1.96; **Table 2**), signifying a concordance of the IF and shale pyrite Co  
427 records, and likely global-scale trends in marine Co concentrations.

428 Higher seawater Co concentrations in the interval between 2.8 and 1.84 Ga reflect  
429 pervasive anoxia and a higher hydrothermal Co flux to the marine reservoir during the  
430 emplacement of oceanic crust, likely due in part to several mantle plume events at this

431 time (Barley et al., 2005; Rasmussen et al., 2012). These events also likely supplied the  
432 Fe for major IF deposited from 2.5 to 2.4 Ga, and again between 2.0 and 1.8 Ga (Barley  
433 et al., 1997; Rasmussen et al., 2012). In hydrothermal systems, the supply of Co tracks  
434 that of Fe (Douville et al., 2002) because the solubility of both elements is enhanced at  
435 higher temperature and Cl<sup>-</sup> concentrations (Metz and Trefry, 2000). Archean-aged  
436 hydrothermal systems are thought to have experienced higher heat flow, enhancing the  
437 supply of Fe (Isley, 1995), and likely Co to seawater. Higher Co concentrations from  
438 Archean hydrothermal fluids are also more likely due to the prevalence of ultramafic  
439 oceanic crust (Arndt, 1983). Compositional control on Co concentrations in  
440 hydrothermal fluids is indicated in the ultramafic Rainbow vent field on the Mid-Atlantic  
441 Ridge, where Co concentrations reach up to 13 μM Co (Douville et al., 2002), an  
442 enrichment of at least 10<sup>5</sup> above seawater concentrations. Persistent anoxia would  
443 have allowed the dispersion of dissolved Co plumes without trapping near source by  
444 oxidative scavenging (Noble et al., 2012). These factors indicate an increased  
445 proportion of hydrothermal Co fluxes relative to continental Co fluxes in comparison to  
446 modern Co inputs (**Table 1**).

447 The Co concentrations in younger than 1.84 Ga IF are comparable to those prior to  
448 2.8 Ga (**Table 2**), potentially indicating that weathering of mafic to ultramafic  
449 Neoproterozoic continental crust is not an essential aspect of the large enrichments. This is  
450 in contrast to Ni, whose supply to oceans from weathering of emergent oceanic  
451 plateaus waned after 2.7-2.6 Ga (Kamber, 2010; Konhauser et al., 2009). Although Co  
452 and Ni have generally similar low-temperature geochemical behavior, they are  
453 decoupled during high-temperature hydrothermal alteration. Nickel is not as efficiently

454 leached as Co, resulting in low hydrothermal Ni fluxes (Douville et al., 2002).  
455 Furthermore, Co-chloride complexes are more stable than Cu-, and, probably, Ni-  
456 chloride complexes, resulting in higher Co solubility at low temperatures (Metz and  
457 Trefry, 2000). The increase in marine sediment Co concentrations after ca. 2.8 Ga may  
458 be driven by changes in the riverine flux of Co from the continents due to increased,  
459 permanent, subaerial exposure. Other authors have suggested the emergence of  
460 continents between 2.9 and 2.7 Ga (e.g. Pons et al., 2013 and references within).  
461 However, the crustal growth rate slows and Co concentrations drop at 2.5 Ga, from 22-  
462 25 ppm to 15 ppm (Condie, 1993), in the midst of the highest sedimentary Co  
463 concentrations (**Fig. 4 and 5**).

464 We propose that the drop in Co concentrations in marine sediments that occurs after  
465 1.84 Ga, and reflects a cessation of hydrothermal activity and the emplacement of large  
466 igneous provinces (Rasmussen et al., 2012). As supply of hydrothermal Fe and  
467 deposition of massive IF waned in the late Paleoproterozoic, so too did the  
468 hydrothermal Co flux, shifting towards modern conditions in which continentally-derived  
469 Co dominates Co influx (**Table 1**). Hydrothermal supply to the oceans reached modern  
470 levels by 0.7-0.8 Ga (Derry and Jacobsen, 1988), with episodic larger mantle inputs re-  
471 occurring throughout the Proterozoic and Phanerozoic (Peng et al., 2011; Veizer et al.,  
472 1983). Additional Middle Proterozoic samples would be needed to test whether later  
473 mantle plume events resulted in a return to globally high marine Co concentrations.

474 The drop in seawater Co concentrations after 1.88 Ga occurs at a time when the  
475 extent of euxinic environments in the oceans increased (Poulton et al., 2004) at the  
476 expense of ferruginous sediments. Without well-constrained depositional rates for IF, it

477 is impossible to estimate Co MAR from ferruginous settings, although our IF dataset  
478 attests to the fact that Co is effectively buried under ferruginous conditions.  
479 Nevertheless, given that IFs are rare marine sediments, the contribution of ferruginous  
480 sediments to overall Co removal in the oceans was likely low. Further, as stressed  
481 above, the Co sink associated with ferruginous settings will be lower than for oxic  
482 sediments; although Fe(III) (oxyhydr)oxides sorb Co, Mn(III/IV) oxides, which form at  
483 higher Eh, are much more effective at scavenging Co from seawater (Stockdale et al.,  
484 2010). Therefore, expansion of euxinic settings to less than 10% of seafloor area in the  
485 Middle Proterozoic (Reinhard et al., 2013), are unlikely to explain the drop in the Co  
486 reservoir size (cf. Saito et al., 2003) without invoking a waning hydrothermal Co source.  
487 Significant areal expansion of oxic *and* euxinic sediments might explain the drop in the  
488 Co reservoir, but oxic conditions suitable for Co scavenging were likely confined to  
489 Middle Proterozoic surface waters (Planavsky et al., 2010a), and sediments deposited  
490 under oxic conditions were of limited extent (Reinhard et al., 2013).

491 The logarithmic range of Co concentrations in sediments, even those from the same  
492 formation, is a phenomenon that has been observed for other trace elements (e.g. Zn;  
493 Robbins et al., 2013; Scott et al., 2012). This variability is likely primary, based on  
494 similar phenomena in modern authigenic sediments (**Fig. 2** and **4**). For Co, this may  
495 reflect temporal variability in marine Co concentrations, which is expected because Co  
496 is a non-conservative element within the oceans and has an extremely short residence  
497 time in seawater, 280 years by our estimate (**Table 1**; 40-120 years; Saito and Moffett,  
498 2002). Due to its short residence time, marine Co concentrations respond quickly to  
499 perturbations in sources or sinks, such as the development of OMZ that fluctuate on

500 decadal time scales (Noble et al., 2012; Stramma et al., 2008). The highest IF Co/Ti  
501 (nearly 160,000  $\mu\text{g g}^{-1}$ ) and pyrite Co (nearly 2000 ppm) are found in the 2.32 Ga  
502 Timeball Hill Formation and the underlying Rooihogte formations. Post-depositional  
503 hydrothermal overprint is not likely responsible for elevated Co concentrations because  
504 they do not correspond to high Pb or Cu, concentrations (data not shown), which would  
505 suggest mineralization. Some of this variation may be primary, and representative of  
506 temporally or spatially variable Co concentrations within the basin. However, some  
507 variability could be tied to re-distribution between Fe-phases during diagenesis. Despite  
508 these variations, the robust statistical differences in time-binned averages (**Table 2**)  
509 validate that shifts in sedimentary Co map onto global events, and hence, indicate  
510 reservoir changes.

511 Although there are no significant changes in the average Co concentrations from  
512 Middle Proterozoic to Phanerozoic in any of the sedimentary records (**Table 2**), there is  
513 significant variability in Phanerozoic euxinic shales (**Fig. 5**), many of which were  
514 deposited during ocean anoxic events (OAE), which reflect transient rather than  
515 pervasive anoxic conditions. The average Co/Al ratios from euxinic black shales  
516 deposited during the Cretaceous OAE-2A at Demerera Rise are ~2X larger than euxinic  
517 sediments deposited before or after (their Fig. 9; Hetzel et al., 2009). This is  
518 dramatically different from other redox-sensitive metals such as Mo and V, whose  
519 restricted supply was exhausted during the OAE, leading to depletions of Mo and V  
520 during the peak of the OAE relative to sediments deposited before and after. Cobalt is  
521 mobilized from anoxic sediments (Noble et al., 2012), and therefore increased Co burial  
522 in euxinic sediments might reflect this greater reservoir during anoxic events, and in fact

523 be a proxy for low-oxygen conditions (Saito et al., 2010). OAE Co enrichments may also  
524 be linked to, or augmented by a hydrothermal Co pulse (e.g. Brumsack, 2006).  
525 Importantly, there is independent evidence for increased hydrothermal input from a  
526 sharp shift toward less radiogenic (hydrothermally-derived) initial Os isotope values  
527 during the onset of the OAE (Turgeon and Creaser, 2008). Furthermore, other authors  
528 have also documented sedimentary Co increases during OAE intervals linked to  
529 hydrothermal activity (Orth et al., 1993; Snow et al., 2005). Therefore, the OAE Co  
530 records are consistent with the notions developed above that anoxia and hydrothermal  
531 activity play a critical role in the global marine Co cycle, and that marine Co  
532 concentrations respond on shorter timescales than conservative elements such as Mo.

533 Surprisingly, we find little evidence for a change in the marine Co reservoir with the  
534 deep ocean oxygenation, potentially beginning as early as 635 Ma (Sahoo et al., 2012).  
535 The average Co/Al ( $\mu\text{g g}^{-1}$ ) for Proterozoic euxinic shales (11.51  $\pm$  1.73) is not  
536 significantly different from Phanerozoic-aged shales (9.33  $\pm$  1.97), although we  
537 emphasize that Phanerozoic shales are dominated by OAE samples, and likely reflect  
538 transient anoxia. There is also no statistical support for changes in IF or shale pyrite Co  
539 concentrations during similar time intervals (data not shown). We note however, that a  
540 paucity of datapoints from the Middle Proterozoic for all three databases hinders  
541 interpretation of changes to the Co reservoir with deep ocean oxygenation. The highest  
542 Phanerozoic Co concentrations occur in exhalites, which demonstrate that near-source  
543 scavenging reactions prevent hydrothermal Co dispersal under oxic conditions, and  
544 therefore Phanerozoic exhalites likely reflect only local Co concentrations. Non-OAE  
545 euxinic shale pyrites would likely best track changes in the Co reservoir associated with

546 ocean oxygenation. Because expanding oxic sediments at the expense of anoxic should  
547 enhance Co removal, and Neoproterozoic hydrothermal activity is likely similar to  
548 modern (Derry and Jacobsen, 1988), ocean ventilation should have further decreased  
549 the Co reservoir size.

550

### 551 *5.3 Marine Cobalt reservoir size and biological evolution*

552 Our empirical record of the marine Co reservoir affords an opportunity to discuss  
553 hypotheses of Co utilization in biology, and to consider how Co-utilization in aquatic  
554 organisms fit to these hypotheses. The biological utilization of metalloproteins may  
555 reflect the availability of elements in the environment in which the protein first appeared  
556 (e.g. Nisbet and Fowler, 1996). Genomic analyses of all three domains of life indicate  
557 that Co-binding proteins originated after 3.3 Ga (David and Alm, 2011). Given the  
558 uncertainties in this age stated by the authors (>250 My), it is feasible that origin of  
559 many Co-binding proteins coincides with the enhanced marine Co availability we  
560 observe after 2.8 Ga, generally supporting the availability hypothesis. However, Co is  
561 chemically suited to catalyze reactions involving hydrogen rather than oxygen (Fraústo  
562 da Silva and Williams, 2001), and any preferential Co utilization by early organisms may  
563 simply reflect the abundance of reduced energy sources such as methane, carbon  
564 monoxide, and hydrogen on the early Earth (Zerkle et al., 2005). Because higher Co  
565 availability is linked to periods in Earth's history when the oceans were anoxic, had on  
566 average lower Co burial rates, higher Co mobility, and probably longer Co residence  
567 times, environmental availability and catalytic suitability may both be reflected in the  
568 utilization of Co in organisms or proteins that evolved early.

569 Consistent with a greater utilization of Co by early organisms, bacteria and archaea  
570 have a greater number of genes that encode for Co-binding proteins (Zhang and  
571 Gladyshev, 2010), and their genomes encode a larger proportion of Co-binding proteins  
572 than eukarya (Dupont et al., 2006). In contrast, a lack of encoded Co-binding proteins in  
573 eukarya should indicate evolution predominantly after 1.8 Ga. This is broadly consistent  
574 with initial diversification of eukaryotes in the middle to late Proterozoic (Knoll et al.,  
575 2007). The persistence of the cobalamin-requiring gene *metH* in eukaryotic  
576 phytoplankton, involved in biosynthesis of the essential amino acid methionine,  
577 suggests that lower marine Co concentrations were not a sufficient selection pressure to  
578 drive loss of the *metH* gene in favor of a cobalamin-independent but less efficient gene  
579 (Bertrand et al., 2013), or that key Co-binding proteins were maintained and few new  
580 Co-binding proteins were acquired during genome expansion. Alternately, the  
581 persistence of *metH* in eukaryotic phytoplankton may reflect a later acquisition (Croft et  
582 al., 2005), and it often occurs in eukaryotic phytoplankton that already contained the  
583 cobalamin-independent gene (Helliwell et al., 2011). Thus, eukaryotic *metH* persistence  
584 may be related to its efficiency rather than Co availability.

585 Enzymes that directly bind Co rather than cobalamin also offer insight into how metal  
586 availability regulates enzyme utilization. Both diatoms and eukaryotic algae can  
587 substitute Co (or Cd) for Zn in the carbonic anhydrase enzyme that interconverts CO<sub>2</sub>  
588 and bicarbonate when Zn concentrations are limiting (Morel et al., 1994; Saito and  
589 Goepfert, 2008). Such substitution may be a strategy for coastal algae to deal with  
590 intense metal drawdown during algal blooms (Saito and Goepfert, 2008), but also  
591 indicates that expression of metal-binding proteins encoded at the genomic level are

592 affected by temporally and spatially variable metal concentrations. The trends in Co  
593 sedimentary records presented here reflect geological control over element delivery and  
594 burial; short-term and spatial variability will therefore not be resolvable with our dataset.  
595 Furthermore, the amount of metal-binding protein expressed (i.e. the metallome) should  
596 fluctuate with physical and chemical conditions and the physiological state of the cell  
597 (Bertrand et al., 2013; Saito et al., 2011). Proteomic records are therefore an important  
598 complement to the genome in understanding why utilization of metal-binding proteins  
599 persist, are lost or acquired as metal concentrations change.

600 Finally, although genomic utilization may reflect availability of metals during  
601 evolution, it can also indicate later adaptations to changing metal abundances. For  
602 instance marine cyanobacteria have an absolute requirement for Co that cannot be met  
603 by other metals (Saito et al., 2002; Sunda and Huntsman, 1995), which again may  
604 reflect evolution in largely anoxic or sulfidic oceans with greater Co availability (Saito et  
605 al., 2003), yet thrive in the oxic oceans where Co concentrations are often less than 40  
606 pM. Cobalt utilization may have persisted in cyanobacteria as Co availability declined  
607 due to the acquisition of Co-binding ligands (Saito and Moffett, 2001; Saito et al., 2005).  
608 The hypothesis that availability dictates utilization implies that the earliest life lacked  
609 strategies for acquisition of metals (Nisbet and Fowler, 1996). However, it is clear that  
610 modern organisms possess strategies to deal with limitation. Thus, the evolutionary  
611 history of metal-acquisition genes may be an important consideration when comparing  
612 metal availability to biological utilization, and many of these proteins are still being  
613 identified (Zhang and Gladyshev, 2010).

614

## 615 **6. Conclusions**

616 Trace elements are proxies for tracking marine redox evolution, but most studies  
617 have focused on metals that partition strongly into anoxic or sulfidic sediments (e.g.,  
618 Mo). For Co, and Fe and Mn, which have short residence times in the modern ocean,  
619 marine concentrations respond dynamically to changes in delivery and removal. High  
620 seawater Co concentrations from ~2.8-1.84 Ga, recorded by IF and authigenic pyrites,  
621 resulted from widespread anoxia and enhanced hydrothermal activity and are probably  
622 linked to Fe fluxes that resulted in the deposition of IF. The marine Co reservoir  
623 decreased after ~1.84 Ga due to waning hydrothermal Co delivery. The expansion of  
624 euxinic sediments at the expense of anoxic sediments, which are a negligible sink for  
625 Co, may have also contributed to the Middle Proterozoic Co reservoir decrease.  
626 Variability of Phanerozoic IF and euxinic shale Co concentrations are linked to localized  
627 hydrothermal activity and/or transient anoxic conditions, and as such obscure any global  
628 changes in the marine Co reservoir associated with deep-water oxidation. Our study of  
629 the concentrations of Co in marine sediments through time reveals a more nuanced  
630 view of the marine Co reservoir through Earth's history than is possible with theoretical  
631 models based on thermodynamic equilibrium (e.g. Saito et al., 2003). This emerging  
632 view of the evolution of the marine Co reservoir through time provides a framework for  
633 interpreting Co availability influenced the acquisition and utilization of Co in biology.

634

635 *Acknowledgements* EDS acknowledges support of the National Science Foundation  
636 (NSF) IRFP and a Deutsche Forschungsgemeinschaft grant. NJP acknowledges support  
637 of the National Science Foundation EAR-PF and NSF ELT program. SVL gratefully

638 acknowledges postdoctoral fellowship support from NSERC and LabexMER. Discovery  
639 Grants and CGS-M from NSERC supported KOK, AB, and LJR, respectively. OR  
640 received support from Europole Mer and IFREMER. SJM was supported by the NASA  
641 Exobiology Program, NASA's Astrobiology Institute Fund for International Cooperation,  
642 the University of Colorado Center for Astrobiology, J.W. Fulbright Foundation, University  
643 of Colorado's Office of the Vice Chancellor for Research, and a sabbatical stay at the  
644 Centre de Recherches Pétrographiques et Géochimiques (CRPG-Nancy). This  
645 manuscript benefitted from helpful discussions with Martin Wille.

646

647 **REFERENCES**

- 648 Algeo, T.J., Maynard, J.B., 2004. Trace-element behavior and redox facies in core  
649 shales of Upper Pennsylvanian Kansas-type cyclothems. *Chemical Geology* 206, 289-  
650 318.
- 651 Anbar, A.D., 2008. Elements and Evolution. *Science* 322, 1481-1483.
- 652 Arndt, N.T., 1983. Role of a thin, komatiite-rich oceanic crust in the Archean plate-  
653 tectonic process. *Geology* 11, 372-375.
- 654 Banerjee, R., Ragsdale, S.W., 2003. The many faces of Vitamin B12: catalysis by  
655 cobalamin-dependent enzymes. *Annual Review of Biochemistry* 72, 209-247.
- 656 Barley, M.E., Bekker, A., Krapež, B., 2005. Late Archean to Early Paleoproterozoic  
657 global tectonics, environmental change and the rise of atmospheric oxygen. *Earth and*  
658 *Planetary Science Letters* 238, 156-171.
- 659 Barley, M.E., Pickard, A.L., Sylvester, P.J., 1997. Emplacement of a large igneous  
660 province as a possible cause of banded iron formation 2.45 billion years ago. *Nature*  
661 385, 55-58.
- 662 Bau, M., Moeller, P., 1993. Rare earth element systematics of the chemically  
663 precipitated component in Early Precambrian iron formations and the evolution of the  
664 terrestrial atmosphere-hydrosphere-lithosphere system. *Geochimica et Cosmochimica*  
665 *Acta* 57, 2239-2249.
- 666 Beak, D.G., Kirby, J.K., Hettiarachchi, G.M., Wendling, L.A., McLaughlin, M.J.,  
667 Khatiwada, R., 2011. Cobalt Distribution and Speciation: Effect of Aging, Intermittent  
668 Submergence, In Situ Rice Roots. *Journal of Environmental Quality* 40, 679-695.
- 669 Bekker, A., Slack, J.F., Planavsky, N., Krapez, B., Hofmann, A., Konhauser, K.O.,  
670 Rouxel, O.J., 2010. Iron Formation: The Sedimentary Product of a Complex Interplay  
671 among Mantle, Tectonic, Oceanic, and Biospheric Processes. *Economic Geology* 105,  
672 467-508.
- 673 Bertrand, E.M., Moran, D.M., McIlvin, M.R., Hoffman, J.M., Allen, A.E., Saito, M.A.,  
674 2013. Methionine synthase interreplacement in diatom cultures and communities:  
675 Implications for the persistence of B12 use by eukaryotic phytoplankton. *Limnol.*  
676 *Oceanogr.* 58, 1431-1450.
- 677 Broecker, W.S., 1971. A kinetic model for the chemical composition of sea water.  
678 *Quaternary Research* 1, 188-207.
- 679 Broecker, W.S., Peng, T.-H., 1982. Tracers in the Sea. Lamont-Doherty Geological  
680 Observatory, Columbia University, Palisades, New York.

- 681 Brumsack, H.-J., 1989. Geochemistry of recent TOC-rich sediments from the Gulf of  
682 California and the Black Sea. *Geologische Rundschau* 78, 851-882.
- 683 Brumsack, H.-J., 2006. The trace metal content of recent organic carbon-rich  
684 sediments: Implications for Cretaceous black shale formation. *Palaeogeography,*  
685 *Palaeoclimatology, Palaeoecology* 232, 344-361.
- 686 Canfield, D.E., Raiswell, R., Bottrell, S., 1992. The reactivity of sedimentary iron  
687 minerals toward sulfide. *American Journal of Science* 292, 659-683.
- 688 Carr, M.H., Turekian, K.K., 1961. The geochemistry of cobalt. *Geochimica et*  
689 *Cosmochimica Acta* 23, 9-60.
- 690 Condie, K.C., 1993. Chemical composition and evolution of the upper continental crust:  
691 Contrasting results from surface samples and shales. *Chemical Geology* 104, 1-37.
- 692 Croft, M.T., Lawrence, A.D., Raux-Deery, E., Warren, M.J., Smith, A.G., 2005. Algae  
693 acquire vitamin B12 through a symbiotic relationship with bacteria. *Nature* 438, 90-93.
- 694 Daskalakis, K.D., Helz, G.R., 1992. Solubility of CdS (Greenockite) in sulfidic waters at  
695 25C. *Environmental Science & Technology* 26, 2462-2468.
- 696 David, L.A., Alm, E.J., 2011. Rapid evolutionary innovation during an Archaean genetic  
697 expansion. *Nature* 469, 93-96.
- 698 Derry, L.A., Jacobsen, S.B., 1988. The Nd and Sr isotopic evolution of Proterozoic  
699 seawater. *Geophysical Research Letters* 15, 397-400.
- 700 Douglas, G.B., Adeney, J.A., 2000. Diagenetic cycling of trace elements in the bottom  
701 sediments of the Swan River Estuary, Western Australia. *Applied Geochemistry* 15,  
702 551-566.
- 703 Douville, E., Charlou, J.L., Oelkers, E.H., Bienvenu, P., Jove Colon, C.F., Donval, J.P.,  
704 Fouquet, Y., Prieur, D., Appriou, P., 2002. The rainbow vent fluids (36°14'N, MAR): the  
705 influence of ultramafic rocks and phase separation on trace metal content in Mid-  
706 Atlantic Ridge hydrothermal fluids. *Chemical Geology* 184, 37-48.
- 707 Dryssen, D., Kremling, K., 1990. Increasing hydrogen sulfide concentration and trace  
708 metal behavior in the anoxic Baltic waters. *Marine Chemistry* 30, 193-204.
- 709 Dupont, C.L., Yang, S., Palenik, B., Bourne, P.E., 2006. Modern proteomes contain  
710 putative imprints of ancient shifts in trace metal geochemistry. *Proceedings of the*  
711 *National Academy of Sciences* 103, 17822-17827.
- 712 Dzombak, D.A., Morel, F.M.M., 1990. *Surface Complexation Modeling: Hydrous Ferric*  
713 *Oxide*. John Wiley & Sons, Inc.

- 714 Elderfield, H., Schultz, A., 1996. Mid-ocean ridge hydrothermal fluxes and the chemical  
715 composition of the ocean. *Annual Review of Earth and Planetary Sciences* 24, 191-224.
- 716 Fraústo da Silva, J.J.R., Williams, R.J.P., 2001. *The biological chemistry of the*  
717 *elements*, 2nd  
718 ed. Oxford University Press, New York.
- 719 Froelich, P.N., Klinkhammer, G.P., Bender, M.L., Luedtke, N.A., Heath, G.R., Cullen, D.,  
720 Dauphin, P., Hammond, D., Hartman, B., Maynard, V., 1979. Early oxidation of organic  
721 matter in pelagic sediments of the eastern equatorial Atlantic: suboxic diagenesis.  
722 *Geochimica et Cosmochimica Acta* 43, 1075-1090.
- 723 Gaillardet, J., Viers, J., Dupre, B., 2003. 5.09 Trace elements in river waters, in: Drever,  
724 J.I. (Ed.), *Surface and Ground Water, Weathering, and Soils*. Elsevier, pp. 225-272.
- 725 German, C.R., Campbell, A.C., Edmond, J.M., 1991. Hydrothermal scavenging at the  
726 Mid-Atlantic Ridge: Modification of trace element dissolved fluxes. *Earth and Planetary*  
727 *Science Letters* 107, 101-114.
- 728 Glassley, W.E., Piper, D.Z., 1978. Cobalt and scandium partitioning versus iron content  
729 for crystalline phases in ultramafic nodules. *Earth and Planetary Science Letters* 39,  
730 173-178.
- 731 Helliwell, K.E., Wheeler, G.L., Leptos, K.C., Goldstein, R.E., Smith, A.G., 2011. Insights  
732 into the Evolution of Vitamin B12 Auxotrophy from Sequenced Algal Genomes.  
733 *Molecular Biology and Evolution* 28, 2921-2933.
- 734 Helz, G.R., Bura-Nakić, E., Mikac, N., Ciglenc̆ki, I., 2011. New model for molybdenum  
735 behavior in euxinic waters. *Chemical Geology* 284, 323-332.
- 736 Hetzel, A., Böttcher, M.E., Wortmann, U.G., Brumsack, H.-J.r., 2009. Paleo-redox  
737 conditions during OAE 2 reflected in Demerara Rise sediment geochemistry (ODP Leg  
738 207). *Palaeogeography, Palaeoclimatology, Palaeoecology* 273, 302-328.
- 739 Ho, T.-Y., Quigg, A., Finkel, Z.V., Milligan, A.J., Wyman, K., Falkowski, P.G., Morel,  
740 F.M.M., 2003. The elemental composition of some marine phytoplankton. *Journal of*  
741 *Phycology* 39, 1145-1159.
- 742 Hrishceva, E., Scott, S.D., 2007. Geochemistry and morphology of metalliferous  
743 sediments and oxyhydroxides from the Endeavour segment, Juan de Fuca Ridge.  
744 *Geochimica et Cosmochimica Acta* 71, 3476-3497.
- 745 Huerta-Diaz, M.A., Morse, J.W., 1992. Pyritization of trace metals in anoxic marine  
746 sediments. *Geochimica et Cosmochimica Acta* 56, 2681-2702.
- 747 Isley, A.E., 1995. Hydrothermal plumes and the delivery of iron to Banded Iron  
748 Formations. *Journal of Geology* 103, 169-185.

- 749 Kamber, B.S., 2010. Archean mafic–ultramafic volcanic landmasses and their effect on  
750 ocean–atmosphere chemistry. *Chemical Geology* 274, 19-28.
- 751 Kamber, B.S., Greig, A., Collerson, K.D., 2005. A new estimate for the composition of  
752 weathered young upper continental crust from alluvial sediments, Queensland,  
753 Australia. *Geochimica et Cosmochimica Acta* 69, 1041-1058.
- 754 Knoll, A.H., Summons, R.E., Waldbauer, J.R., Zumberge, J.E., 2007. The geological  
755 succession of primary producers in the oceans., in: Falkowski, P.G., Knoll, A.H. (Eds.),  
756 *Evolution of Primary Producers in the Sea*. Elsevier, Boston, pp. 133-163.
- 757 Konhauser, K.O., Lalonde, S.V., Amskold, L., Holland, H.D., 2007. Was There Really an  
758 Archean Phosphate Crisis? *Science* 315, 1234.
- 759 Konhauser, K.O., Lalonde, S.V., Planavsky, N.J., Pecoits, E., Lyons, T.W., Mojzsis,  
760 S.J., Rouxel, O.J., Barley, M.E., Rosiere, C., Fralick, P.W., Kump, L.R., Bekker, A.,  
761 2011. Aerobic bacterial pyrite oxidation and acid rock drainage during the Great  
762 Oxidation Event. *Nature* 478, 369-373.
- 763 Konhauser, K.O., Newman, D.K., Kappler, A., 2005. The potential significance of  
764 microbial Fe(III) reduction during deposition of Precambrian banded iron formations.  
765 *Geobiology* 3, 167-177.
- 766 Konhauser, K.O., Pecoits, E., Lalonde, S.V., Papineau, D., Nisbet, E.G., Barley, M.E.,  
767 Arndt, N.T., Zahnle, K., Kamber, B.S., 2009. Oceanic nickel depletion and a  
768 methanogen famine before the Great Oxidation Event. *Nature* 458, 750-753.
- 769 Koschinsky, A., Hein, J.R., 2003. Uptake of elements from seawater by ferromanganese  
770 crusts: solid-phase associations and seawater speciation. *Marine Geology* 198, 331-  
771 351.
- 772 Krauskopf, K.B., 1956. Factors controlling the concentrations of thirteen rare metals in  
773 sea-water. *Geochimica et Cosmochimica Acta* 9, 1-32.
- 774 Kremling, K., 1983. The behavior of Zn, Cd, Cu, Ni, Co, Fe, and Mn in anoxic baltic  
775 waters. *Marine Chemistry* 13, 87-108.
- 776 Krishnaswami, S., 1976. Authigenic transition elements in Pacific pelagic clays.  
777 *Geochimica et Cosmochimica Acta* 40, 425-434.
- 778 Limpert, E., Stahel, W.A., Abbt, M., 2001. Log-normal Distributions across the Sciences:  
779 Keys and Clues. *BioScience* 51, 341-352.
- 780 Lyons, T.W., Werne, J.P., Hollander, D.J., Murray, R.W., 2003. Contrasting sulfur  
781 geochemistry and Fe/Al and Mo/Al ratios across the last oxic-to-anoxic transition in the  
782 Cariaco Basin, Venezuela. *Chemical Geology* 195, 131-157.

- 783 Manceau, A., Drits, V.A., Silvester, E., Bartoli, C., Lanson, B., 1997. Structural  
784 mechanism of Co<sup>2+</sup> oxidation by the phylломanganate buserite. *American Mineralogist*  
785 82, 1150-1175.
- 786 Metz, S., Trefry, J.H., 2000. Chemical and mineralogical influences on concentrations of  
787 trace metals in hydrothermal fluids. *Geochimica et Cosmochimica Acta* 64, 2267-2279.
- 788 Moffett, J.W., Ho, J., 1996. Oxidation of cobalt and manganese in seawater via a  
789 common microbially catalyzed pathway. *Geochimica et Cosmochimica Acta* 60, 3415-  
790 3424.
- 791 Morel, F.M.M., Reinfelder, J.R., Roberts, S.B., Chamberlain, C.P., Lee, J.G., Yee, D.,  
792 1994. Zinc and carbon co-limitation of marine phytoplankton. *Nature* 369, 740-742.
- 793 Morse, J.W., Arakaki, T., 1993. Adsorption and coprecipitation of divalent metals with  
794 mackinawite (FeS). *Geochimica et Cosmochimica Acta* 57, 3635-3640.
- 795 Morse, J.W., Luther III, G.W., 1999. Chemical influences on trace metal-sulfide  
796 interactions in anoxic sediments. *Geochimica et Cosmochimica Acta* 63, 3373-3378.
- 797 Murray, J.W., Dillard, J.G., 1979. The oxidation of cobalt(II) adsorbed on manganese  
798 dioxide. *Geochimica et Cosmochimica Acta* 43, 781-787.
- 799 Murray, K.J., Webb, S.M., Bargar, J.R., Tebo, B.M., 2007. Indirect Oxidation of Co(II) in  
800 the Presence of the Marine Mn(II)-Oxidizing Bacterium *Bacillus* sp. Strain SG-1. *Applied*  
801 *and Environmental Microbiology* 73, 6905-6909.
- 802 Musić, S., Gessner, M., Wolf, R.H.H., 1979. Sorption of small amounts of cobalt(II) on  
803 iron(III) oxide. *Microchimica Acta* 71, 105-112.
- 804 Nisbet, E.G., Fowler, C.M.R., 1996. The hydrothermal imprint on life: did heat-shock  
805 proteins, metalloproteins and photosynthesis begin around hydrothermal vents?  
806 *Geological Society, London, Special Publications* 118, 239-251.
- 807 Noble, A.E., Lamborg, C.H., Ohnemus, D.C., Lam, P.J., Goepfert, T.J., Measures, C.I.,  
808 Frame, C.H., Casciotti, K.L., DiTullio, G.R., Jennings, J., Saito, M.A., 2012. Basin-scale  
809 inputs of cobalt, iron, and manganese from the Benguela-Angola front to the South  
810 Atlantic Ocean. *Limnol. Oceanogr.* 57, 989-1010.
- 811 Noble, A.E., Saito, M.A., Maiti, K., Benitez-Nelson, C.R., 2008. Cobalt, manganese, and  
812 iron near the Hawaiian Islands: A potential concentrating mechanism for cobalt within a  
813 cyclonic eddy and implications for the hybrid-type trace metals. *Deep-Sea Research II*  
814 55, 1473-1490.
- 815 Orth, C.J., Attrep Jr, M., Quintana, L.R., Elder, W.P., Kauffman, E.G., Diner, R., Villamil,  
816 T., 1993. Elemental abundance anomalies in the late Cenomanian extinction interval: a  
817 search for the source(s). *Earth and Planetary Science Letters* 117, 189-204.

- 818 Öztürk, M., 1995. Trends of trace metal (Mn, Fe, Co, Ni, Cu, Zn, Cd and Pb)  
819 distributions at the oxic-anoxic interface in sulfidic water of the Drammensjord. *Marine*  
820 *Chemistry* 48, 329-342.
- 821 Peng, P., Bleeker, W., Ernst, R.E., Söderlund, U., McNicoll, V., 2011. U–Pb baddeleyite  
822 ages, distribution and geochemistry of 925 Ma mafic dykes and 900 Ma  
823 sills in the North China craton: Evidence for a Neoproterozoic mantle plume. *Lithos* 127,  
824 210-221.
- 825 Piper, D.Z., Dean, W.E., 2002. Trace element deposition in the Cariaco Basin,  
826 Venezuela shelf, under sulfate-reducing conditions - a history of the local hydrography  
827 and global climate, 20 ka to the present, USGS Professional Paper, p. 45 pp.
- 828 Planavsky, N., Bekker, A., Rouxel, O.J., Kamber, B., Hofmann, A., Knudsen, A., Lyons,  
829 T.W., 2010a. Rare Earth Element and yttrium compositions of Archean and  
830 Paleoproterozoic Fe formations revisited: New perspectives on the significance and  
831 mechanisms of deposition. *Geochimica et Cosmochimica Acta* 74, 6387-6405.
- 832 Planavsky, N.J., McGoldrick, P., Scott, C.T., Li, C., Reinhard, C.T., Kelly, A.E., Chu, X.,  
833 Bekker, A., Love, G.D., Lyons, T.W., 2011. Widespread iron-rich conditions in the mid-  
834 Proterozoic ocean. *Nature* 477, 448-451.
- 835 Planavsky, N.J., Rouxel, O.J., Bekker, A., Lalonde, S.V., Konhauser, K.O., Reinhard,  
836 C.T., Lyons, T.W., 2010b. The evolution of the marine phosphate reservoir. *Nature* 467,  
837 1088-1090.
- 838 Pons, M.L., Fujii, T., Rosing, M., Quitté, G., Télouk, P., Albarède, F., 2013. A Zn isotope  
839 perspective on the rise of continents. *Geobiology* 11, 201-214.
- 840 Poulton, S.W., Fralick, P.W., Canfield, D.E., 2004. The transition to a sulphidic ocean  
841 ~1.84 billion years ago. *Nature* 431, 173-177.
- 842 Rasmussen, B., Buick, R., 1999. Redox state of the Archean atmosphere: Evidence  
843 from detrital heavy minerals in ca. 3250–2750 Ma sandstones from the Pilbara Craton,  
844 Australia. *Geology* 27, 115-118.
- 845 Rasmussen, B., Fletcher, I.R., Bekker, A., Muhling, J.R., Gregory, C.J., Thorne, A.M.,  
846 2012. Deposition of 1.88-billion-year-old iron formations as a consequence of rapid  
847 crustal growth. *Nature* 484, 498-501.
- 848 Reinhard, C.T., Planavsky, N.J., Robbins, L.J., Partin, C.A., Gill, B.C., Lalonde, S.V.,  
849 Bekker, A., Konhauser, K.O., Lyons, T.W., 2013. Proterozoic ocean redox and  
850 biogeochemical stasis. *Proceedings of the National Academy of Sciences*.
- 851 Robbins, L.J., Lalonde, S.V., Saito, M.A., Planavsky, N.J., Mloszewska, A.M., Pecoits,  
852 E., Scott, C., Dupont, C.L., Kappler, A., Konhauser, K.O., 2013. Authigenic iron oxide  
853 proxies for marine zinc over geological time and implications for marine eukaryotic  
854 metallome evolution. *Geobiology* 11, 295-306.

- 855 Rouxel, O.J., Bekker, A., Edwards, K.J., 2005. Iron Isotope Constraints on the Archean  
856 and Paleoproterozoic Ocean Redox State. *Science* 307, 1088-1091.
- 857 Rouxel, O.J., Bekker, A., Edwards, K.J., 2006. Response to Comment on "Iron Isotope  
858 Constraints on the Archean and Paleoproterozoic Ocean Redox State. *Science* 311.
- 859 Sahoo, S.K., Planavsky, N.J., Kendall, B., Wang, X., Shi, X., Scott, C., Anbar, A.D.,  
860 Lyons, T.W., Jiang, G., 2012. Ocean oxygenation in the wake of the Marinoan  
861 glaciation. *Nature* 489, 546-549.
- 862 Saito, M.A., Bertrand, E.M., Dutkiewicz, S., Bulygin, V.V., Moran, D.M., Monteiro, F.M.,  
863 Follows, M.J., Valois, F.W., Waterbury, J.B., 2011. Iron conservation by reduction of  
864 metalloenzyme inventories in the marine diazotroph *Crocospaera watsonii*.  
865 *Proceedings of the National Academy of Sciences* 108, 2184-2189.
- 866 Saito, M.A., Goepfer, T.J., Noble, A.E., Bertrand, E.M., Sedwick, P.N., DiTullio, G.R.,  
867 2010. A seasonal study of dissolved cobalt in the Ross Sea, Antarctica: micronutrient  
868 behavior, absence of scavenging, and relationships with Zn, Cd, and P. *Biogeosciences*  
869 7, 4059-4082.
- 870 Saito, M.A., Goepfert, T.J., 2008. Zinc-cobalt colimitation of *Phaeocystis antarctica*.  
871 *Limnol. Oceanogr.* 53, 266-275.
- 872 Saito, M.A., Moffett, J.W., 2001. Complexation of cobalt by natural organic ligands in the  
873 Sargasso Sea as determined by a new high-sensitivity electrochemical cobalt speciation  
874 method suitable for open ocean work. *Marine Chemistry* 75, 49-68.
- 875 Saito, M.A., Moffett, J.W., 2002. Temporal and spatial variability of cobalt in the Atlantic  
876 Ocean. *Geochimica et Cosmochimica Acta* 66, 1943-1953.
- 877 Saito, M.A., Moffett, J.W., Chisholm, S.W., Waterbury, J.B., 2002. Cobalt limitation and  
878 uptake in *Prochlorococcus*. *Limnology and Oceanography* 47, 1629-1636.
- 879 Saito, M.A., Moffett, J. W. and G. R. DiTullio, 2004. Cobalt and nickel in the Peru  
880 upwelling region: A major flux of labile cobalt utilized as a micronutrient. *Global*  
881 *Biogeochemical Cycles* 18.
- 882 Saito, M.A., Noble, A.E., Tagliabue, A., Goepfert, T.J., Lamborg, C.H., Jenkins, W.J.,  
883 2013. Slow-spreading submarine ridges in the South Atlantic as a significant oceanic  
884 iron source. *Nature Geosci* 6, 775-779.
- 885 Saito, M.A., Rocap, G., Moffett, J.W., 2005. Production of cobalt binding ligands in a  
886 *Synechococcus* feature at the Costa Rica upwelling dome. *Limnology and*  
887 *Oceanography* 50, 279-290.
- 888 Saito, M.A., Sigman, D.M., Morel, F.M.M., 2003. The bioinorganic chemistry of the  
889 ancient ocean: the co-evolution of the cyanobacterial metal requirements and

- 890 biogeochemical cycles at the Archean-Paleoproterozoic boundary? *Inorganica Chimica*  
891 *Acta* 356, 308-318.
- 892 Sander, S.G., Koschinsky, A., 2011. Metal flux from hydrothermal vents increased by  
893 organic complexation. *Nature Geoscience* 4, 145-150.
- 894 Scott, C., Lyons, T.W., 2012. Contrasting molybdenum cycling and isotopic properties in  
895 euxinic versus non-euxinic sediments and sedimentary rocks: Refining the  
896 paleoproxies. *Chemical Geology* 324-325, 19-27.
- 897 Scott, C., Lyons, T.W., Bekker, A., Shen, Y., Poulton, S.W., Chu, X., Anbar, A.D., 2008.  
898 Tracing the stepwise oxygenation of the Proterozoic ocean. *Nature* 452, 456-459.
- 899 Scott, C., Planavsky, N.J., Dupont, C.L., Kendall, B., Gill, B.C., Robbins, L.J., Husband,  
900 K.F., Arnold, G.L., Wing, B.A., Poulton, S.W., Bekker, A., Anbar, A.D., Konhauser, K.O.,  
901 Lyons, T.W., 2012. Bioavailability of zinc in marine systems through time. *Nature*  
902 *Geoscience* 6, 125-128.
- 903 Shelley, R.U., Sedwick, P.N., Bibby, T.S., Cabedo-Sanz, P., Church, T.M., Johnson,  
904 R.J., Macey, A.I., Marsay, C.M., Sholkovitz, E.R., Ussher, S.J., Worsfold, P.J., Lohan,  
905 M.C., 2012. Controls on dissolved cobalt in surface waters of the Sargasso Sea:  
906 Comparisons with iron and aluminum. *Global Biogeochem. Cycles* 26.
- 907 Snow, L.J., Duncan, R.A., Bralower, T.J., 2005. Trace element abundances in the Rock  
908 Canyon Anticline, Pueblo, Colorado, marine sedimentary section and their relationship  
909 to Caribbean plateau construction and oxygen anoxic event 2. *Paleoceanography* 20,  
910 PA3005.
- 911 Stockdale, A., Davison, W., Zhang, H., Hamilton-Taylor, J., 2010. The association of  
912 cobalt with iron and manganese (oxyhydr)oxides in marine sediment. *Aquatic*  
913 *Geochemistry* 16, 575-585.
- 914 Stramma, L., Johnson, G.C., Sprintall, J., Mohrholz, V., 2008. Expanding Oxygen-  
915 Minimum Zones in the Tropical Oceans. *Science* 320, 655-658.
- 916 Sunda, W.G., Huntsman, S.A., 1995. Cobalt and Zinc Interreplacement in Marine  
917 Phytoplankton: Biological and Geochemical Implications. *Limnology and Oceanography*  
918 40, 1404-1417.
- 919 Tagliabue, A., Bopp, L., Dutay, J.-C., Bowie, A.R., Chever, F., Jean-Baptiste, P.,  
920 Bucciarelli, E., Lannuzel, D., Remenyi, T., Sarthou, G., Aumont, O., Gehlen, M.,  
921 Jeandel, C., 2010. Hydrothermal contribution to the oceanic dissolved iron inventory.  
922 *Nature Geosci* 3, 252-256.
- 923 Takahashi, Y., Manceau, A., Geoffroy, N., Marcus, M.A., Usui, A., 2007. Chemical and  
924 structural control of the partitioning of Co, Ce, and Pb in marine ferromanganese oxides.  
925 *Geochimica et Cosmochimica Acta* 71, 984-1008.

- 926 Toner, B.M., Fakra, S.C., Manganini, S.J., Santelli, C.M., Marcus, M.A., Moffett, J.W.,  
927 Rouxel, O., German, C.R., Edwards, K.J., 2009. Preservation of iron(II) by carbon-rich  
928 matrices in a hydrothermal plume. *Nature Geosciences* 2, 197-201.
- 929 Turgeon, S.C., Creaser, R.A., 2008. Cretaceous oceanic anoxic event 2 triggered by a  
930 massive magmatic episode. *Nature* 454, 323-326.
- 931 Van der Weijden, C.H., 2002. Pitfalls of normalization of marine geochemical data using  
932 a common divisor. *Marine Geology* 184, 167-187.
- 933 van der Weijden, C.H., Reichart, G.-J., van Os, B.J.H., 2006. Sedimentary trace  
934 element records over the last 200 kyr from within and below the northern Arabian Sea  
935 oxygen minimum zone. *Marine Geology* 231, 69-88.
- 936 Veizer, J., Compston, W., Clauer, N., Schidlowski, M., 1983.  $^{87}\text{Sr}/^{86}\text{Sr}$  in Late  
937 Proterozoic carbonates: evidence for a "mantle" event at ~900 Ma ago. *Geochimica et*  
938 *Cosmochimica Acta* 47, 295-302.
- 939 Viollier, E., Jézéquel, D., Michard, G., Pèpe, M., Sarazin, G., Albéric, P., 1995.  
940 Geochemical study of a crater lake (Pavin Lake, France): trace-element behaviour in  
941 the monimolimnion. *Chemical Geology* 125, 61-72.
- 942 Wedephol, K.H., 1971. Environmental influences on the chemical composition of shales  
943 and clays, in: Ahrens, L.H., Press, F., Runcorn, S.K., Urey, H.C. (Eds.), *Physics and*  
944 *Chemistry of the Earth*. Pergamon Press, Oxford, United Kingdom, pp. 307-333.
- 945 Wheat, C.G., Jannasch, H.W., Kastner, M., Plant, J.N., DeCarlo, E.H., 2003. Seawater  
946 transport and reaction in upper oceanic basaltic basement: chemical data from  
947 continuous monitoring of sealed boreholes in a ridge flank environment. *Earth and*  
948 *Planetary Science Letters* 216, 549-564.
- 949 Yee, N., Fein, J.B., 2003. Quantifying Metal Adsorption onto Bacteria Mixtures: A Test  
950 and Application of the Surface Complexation Model. *Geomicrobiology Journal* 20, 43.
- 951 Yucel, M., Gartman, A., Chan, C.S., Luther, G.W., 2011. Hydrothermal vents as a  
952 kinetically stable source of iron-sulphide-bearing nanoparticles to the ocean. *Nature*  
953 *Geoscience* 4, 367-371.
- 954 Zerkle, A.L., House, C.H., Brantley, S.L., 2005. Biogeochemical signatures through time  
955 as inferred from whole microbial genomes. *American Journal of Science* 305, 467-502.
- 956 Zhang, Y., Gladyshev, V.N., 2010. General Trends in Trace Element Utilization  
957 Revealed by Comparative Genomic Analyses of Co, Cu, Mo, Ni, and Se. *The Journal of*  
958 *Biological Chemistry* 285, 3393-3405.  
959  
960

961 **Figures and Tables**

962 **Fig. 1. a.** Speciation diagram of Co (white) and Fe in varying Eh-pH conditions.  $\text{Co}^{2+}$  is  
963 stable under marine Eh and pH conditions (i.e. 7-8) inferred for the Precambrian ocean.  
964 In the absence of carbonate,  $\text{Fe}^{2+}$  is soluble. **b.** Speciation diagram of Co (white) and  
965 Mn, showing the similar redox potential for Mn(II) and Co(II) oxidation, which are both  
966 higher than that of Fe(II) oxidation.

967 **Fig. 2.** Co-precipitation of Co with Fe (oxyhydr)oxides can be inferred based on a  
968 correlation coefficient of 0.763 from previously published data from hydrothermal  
969 sediments at the Endeavor Segment, Juan de Fuca Ridge (Hrshceva and Scott, 2007).

970 **Fig. 3.** Sorption of  $\text{Co}^{2+}$  to strong >(s) and weak >(w) surface sites on ferrihydrite in  
971 seawater when **a.** no organic Co-ligands are present, **b.** modern (40 pM) concentrations  
972 of organic ligands (dashed line) are present, and **c.** for an extreme case of 400 pM of  
973 organic ligands.

974 **Fig. 4.** The Co/Ti of IF (symbols) and of evolving continental crust (black line; Condie,  
975 1993). Data points are from bulk (squares) and laser-ablation (circles) analyses of  
976 Precambrian Superior-type IF (red) and Algoma-type IF (black). Also included are  
977 Phanerozoic shallow-marine ironstones (blue) and hydrothermal and exhalative  
978 deposits (green). Data points with >0.5 wt% Mn have been excluded from this  
979 compilation.

980 **Fig. 5.** Cobalt concentrations in pyrite (circles) from modern (open) and ancient (filled)  
981 euxinic shales, and bulk euxinic shales (squares). For reference, the crustal evolution  
982 trend (solid line) is included, based on the Restoration Model of Condie (1993). Modern

983 pyrite Co concentrations from coastal sediments reflect high concentrations of trace  
984 metals delivered from rivers and petroleum reservoirs (Huerta-Diaz and Morse, 1992).

985

**Table 1. Modern Cobalt Budget**

---

<i>Sources</i>		
Riverine Flux	$5.5 \times 10^{12}$	$\text{g kyr}^{-1}$
Hydrothermal Flux	$1.3 \times 10^{11}$	$\text{g kyr}^{-1}$
Oceanic Reservoir Mass	$1.6 \times 10^{12}$	$\text{g}$
Residence Time	0.28	$\text{kyr}$
<i>Sinks</i>		
Oxic MAR	2.3-5	$\mu\text{g Co cm}^{-2} \text{ kyr}^{-1}$
Euxinic MAR	5	$\mu\text{g Co cm}^{-2} \text{ kyr}^{-1}$

---

986

987

988

989

990

991

992

993

994

995

**Table 2.** Statistical differences between Cobalt concentrations in sediments by age bin.

*Iron Formations*

Age Bin	Mean Co/Al ( $\mu\text{g g}^{-1}$ )	*/ SD	<i>p-value</i> *
$\geq 2.80$ Ga	79.85	1.72	
2.75 to 1.88 Ga	150.57	2.67	<0.0001
$\leq 1.72$ Ga	62.25	1.84	<0.0001

*Euxinic Shale Pyrite*

Age Bin	Mean Co (ppm)	*/ SD	<i>p-value</i> *
2.80 to 1.84 Ga	7.34	1.77	
1.80 to 0.30 Ga	3.87	1.96	<0.0001

*Euxinic Shale*

Age Bin	Mean Co/Ti ( $\mu\text{g g}^{-1}$ )	*/ SD	<i>p-value</i> *
$\geq 0.695$ Ga	11.51	1.73	
$\leq 0.531$ Ga	9.33	1.97	0.0842

\**p-values* refer to comparison between the age bin indicated and the preceding age bin.

996

997 **Supplementary Figures and Tables**

998 **Supplementary Table 1.** Co, Ti, Fe, and Mn concentrations and the source of the data  
 999 for the iron-formation samples used in this study.

1000 **Supplementary Table 2.** Co concentrations and the source of the data for pyrite and  
 1001 bulk shale analyses used in this study.

1002 **Supplementary references**

Figure 1

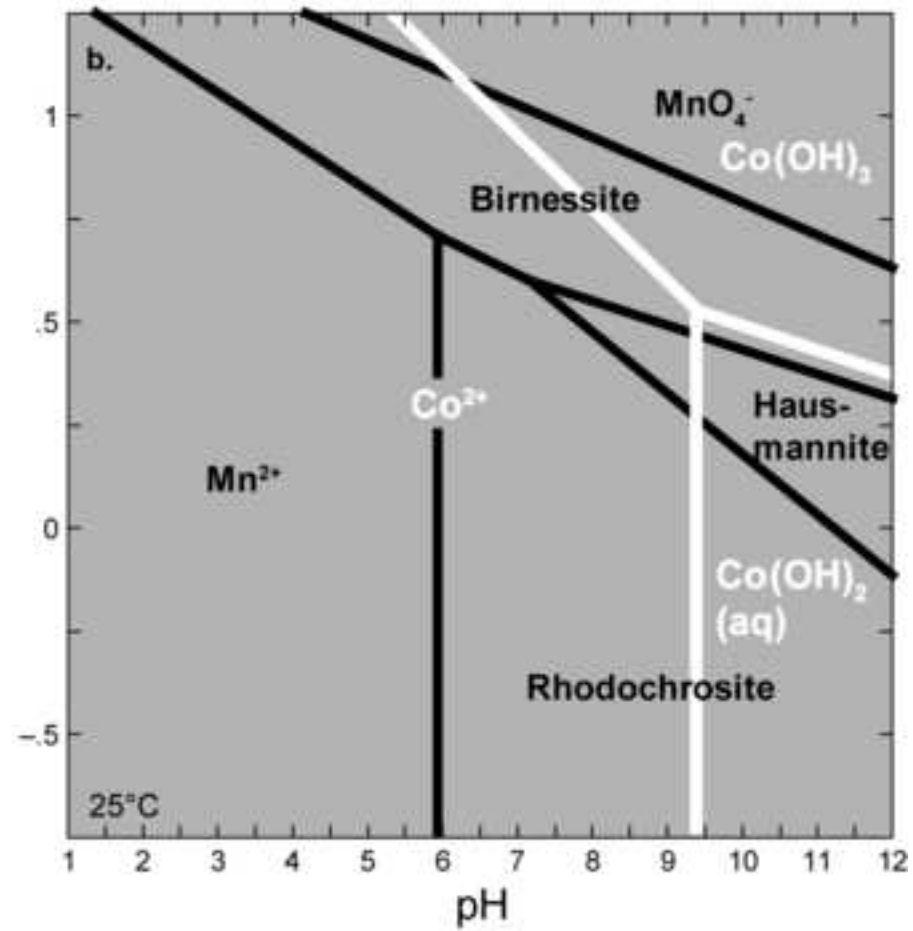
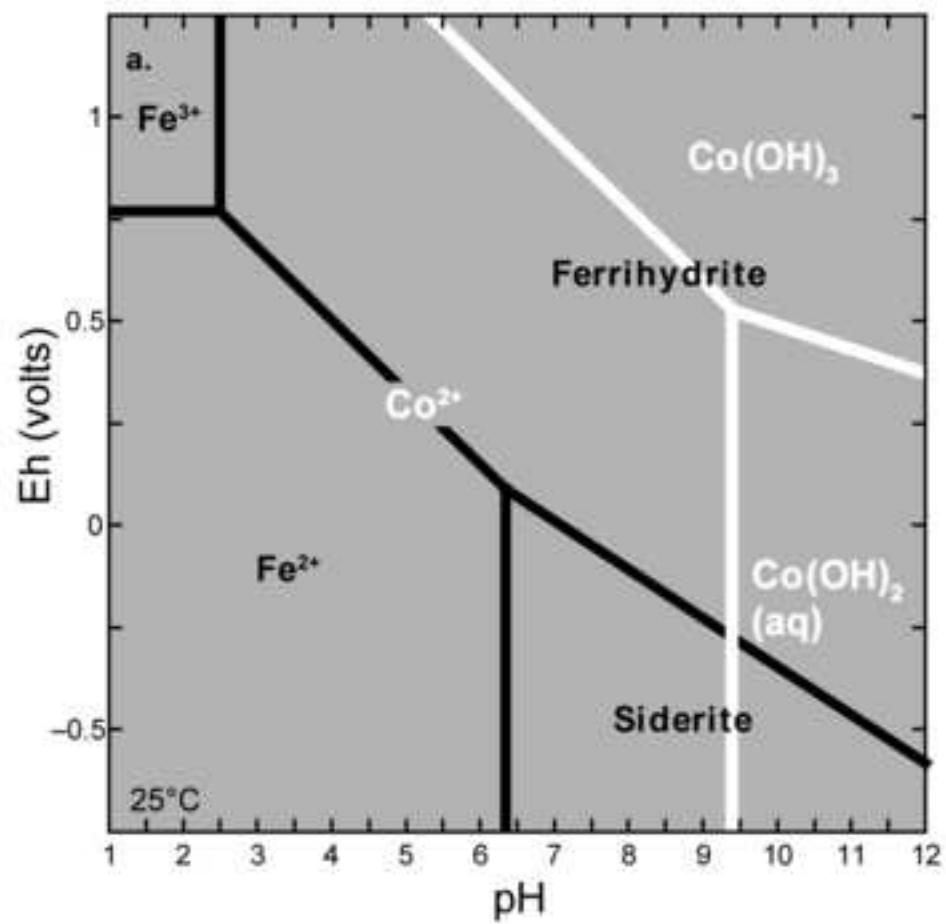


# Figure 2.

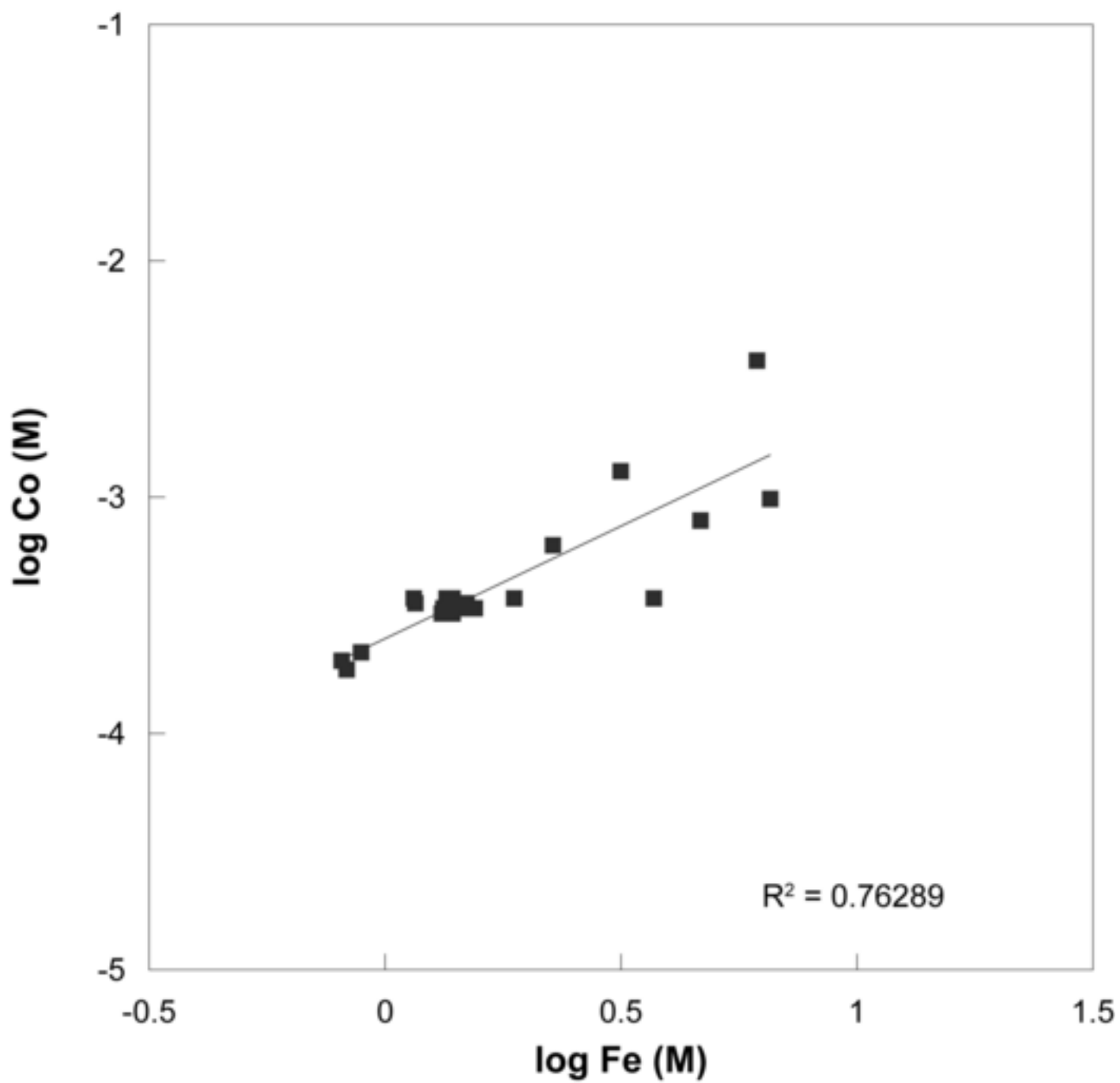


Figure 3

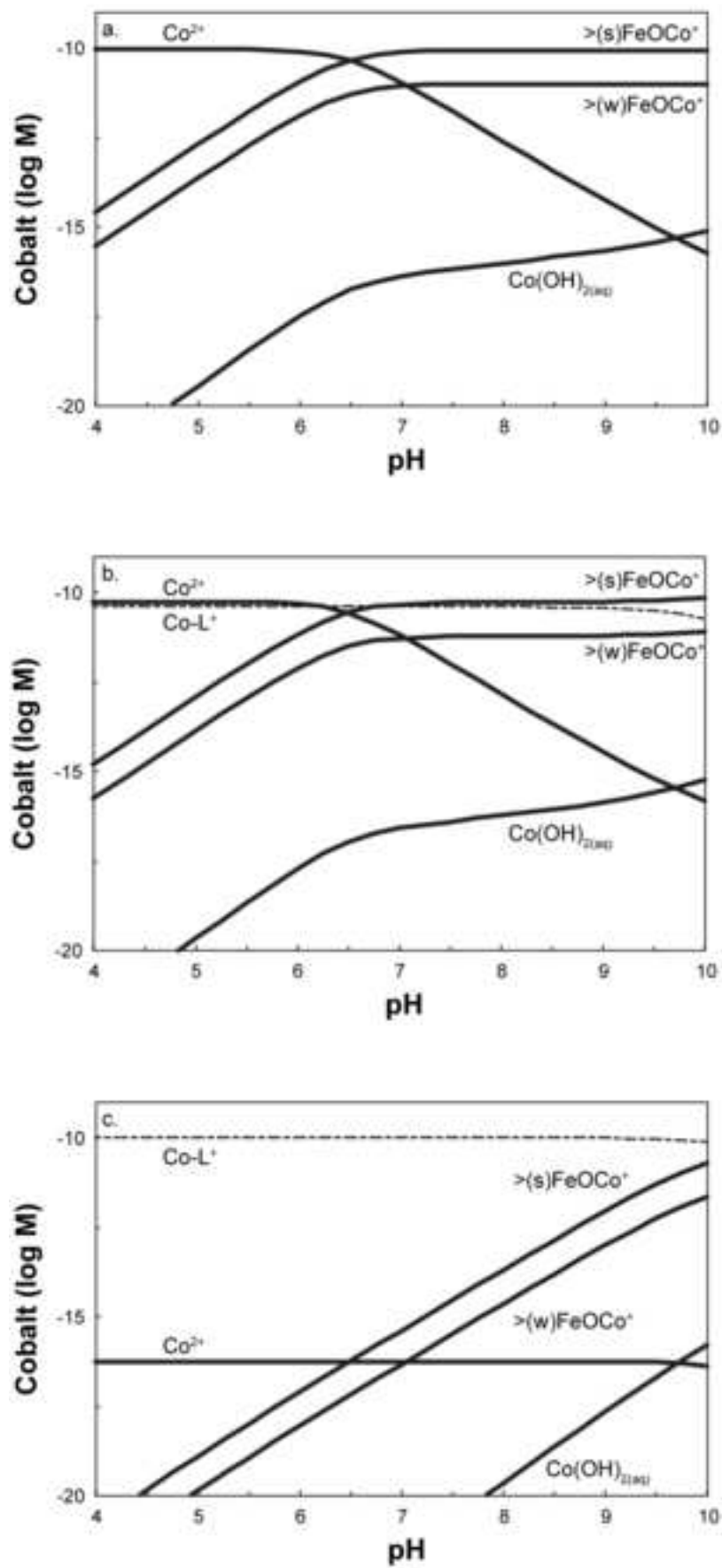


Figure 4.

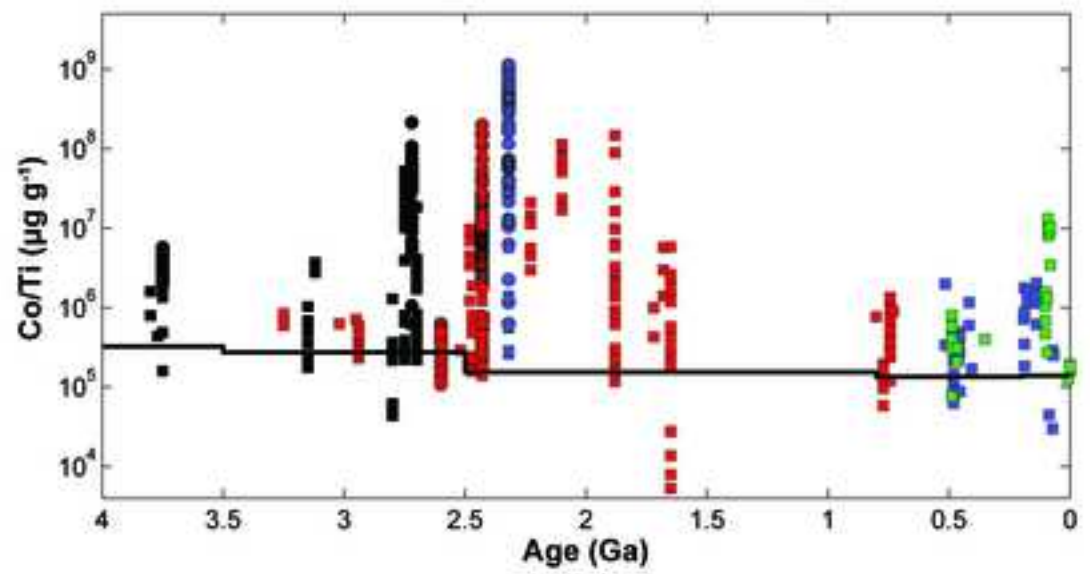
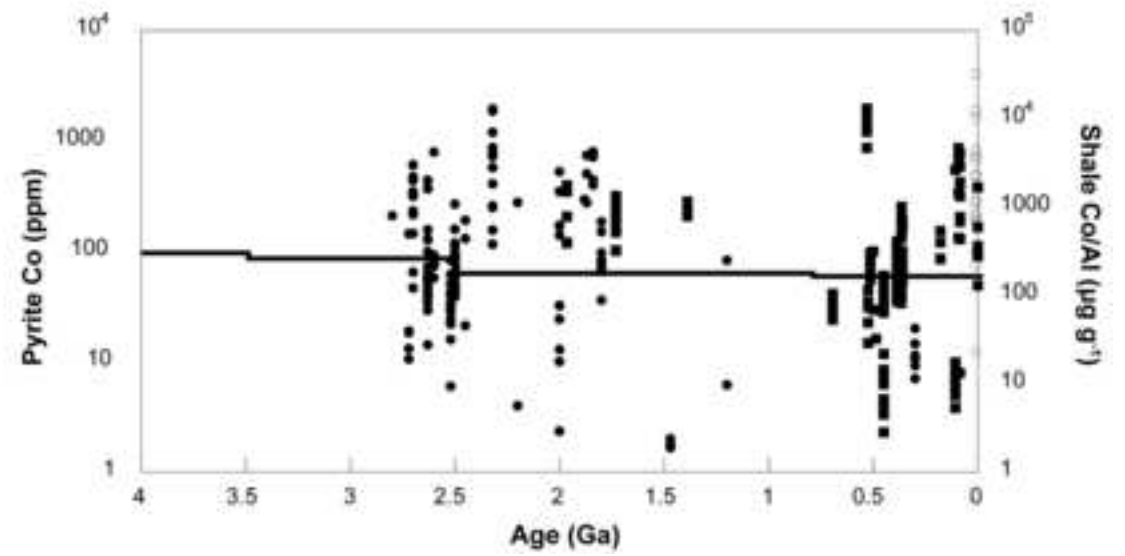


Figure 5.



**Table 1. Modern Cobalt Budget**

---

*Sources*

Riverine Flux	$5.5 \times 10^{12}$	$\text{g kyr}^{-1}$
---------------	----------------------	---------------------

Hydrothermal Flux	$1.3 \times 10^{11}$	$\text{g kyr}^{-1}$
-------------------	----------------------	---------------------

Oceanic Reservoir Mass	$1.6 \times 10^{12}$	$\text{g}$
Residence Time	0.28	$\text{kyr}$

*Sinks*

Oxic MAR	2.3-5	$\mu\text{g Co cm}^{-2} \text{ kyr}^{-1}$
----------	-------	---

Euxinic MAR	5	$\mu\text{g Co cm}^{-2} \text{ kyr}^{-1}$
-------------	---	---

---

**Supplementary references**

[Click here to download Supplementary material for on-line publication only: Supplementary\\_Table1\\_references.doc](#)